Commission of the European Communities

JOINT
RESEARCH
CENTRE

NEANDC (E) 302 "U" Vol. III Euratom
INDC (EUR) 023/G

ANNUAL PROGRESS REPORT ON NUCLEAR DATA 1988

CENTRAL BUREAU FOR NUCLEAR MEASUREMENTS

GEEL (BELGIUM)

June 1989

Commission of the European Communities

JOINT
RESEARCH
CENTRE

NEANDC (E) 302 "U" Vol. III Euratom
INDC (EUR) 023/G

ANNUAL PROGRESS REPORT ON NUCLEAR DATA 1988

CENTRAL BUREAU FOR NUCLEAR MEASUREMENTS

GEEL (BELGIUM)

June 1989

TABLE OF CONTENTS

Editor : H.H. Hansen

Note : For further information concerning the Project Nuclear Measurements (Nuclear Data, Nuclear Metrology), please contact A.J. Deruytter, Project Manager.

EXECUTIVE SUMMARY

A.J. Deruytter

In the 1988-1991 multiannual research programme the project Nuclear Measurements is concerned with Nuclear Data and Nuclear Metrology.
In 1988 the efforts for the improvement of the set of standard neutron cross-sections and other quantities selected within the INDC/NEANDC Standards File continued. The energy spectrum and the fraction of scission neutrons in the spontaneous fission of ^{252}Cf could be deduced for the first time. The average energy of the scission neutrons is (0.39 ± 0.06) MeV and the fraction of scission neutrons with respect to the total amount of prompt neutrons is (1.1 ± 0.3) %.
In the field of nuclear data for fission technology work was concentrated on European requests in the NEA High Priority Request List. In the subthermal energy region fission cross-section measurements for ^{233}U, ^{235}U and ^{239}Pu led to a much improved data base and Westcott g_f-factors. Because of the difficulty of background determinations at GELINA, η of ^{235}U was remeasured with a chopper system at ILL Grenoble. The data are being analysed. The subthermal capture data for ^{238}U are in agreement with a 1/v dependence of this cross section. Mass and energy distributions of fission fragments in the spontaneous fission of the plutonium isotopes could be satisfactorily explained on the basis of fission channels in the random neck-rupture model.
Further efforts to clarify the reasons for the difference between experimental and calculated weighting functions for C_6D_6 detectors used in capture experiments continued in the frame of the NEANDC Task Force. Discontinuities in the level spacings for the neutron resonances in even chromium isotopes were reported and the measurements on nickel isotopes continued.
In the area of nuclear data for fusion technology, the measurements aim at an improvement of relevant data for neutron transport calculations in the blanket and for prediction of gas production. In 1988 excitation functions were measured for the (n,p) and (n,α) reactions in the molybdenum isotopes, an important component of structural materials. This was a collaboration with KFA Jülich . Also the excitation function of the

(n,2n)-reaction for ^{52}Cr, a structural material nuclide, was experimentally determined. Double differential (n,α) cross-section ratios were measured for nickel and copper relative to ^{58}Ni with 14 MeV neutrons with a multitelescope detector. A novel telescope with additional discrimination by time-of-flight was developed to remove remaining discrepancies. Double differential neutron emission cross-section measurements of ^{9}Be will be restarted in 1989 after installation of a U-Be target at GELINA, enabling measurements up to higher neutron energies.
The radionuclide metrology follows three lines: determination of decay-scheme data, preparation of special standards and the improvement of measurement techniques including international comparisons. CBNM participated with four different measuring systems in a BIPM comparison of activity-concentration measurements of a ^{125}I solution. An interactive version of the CBNM code for analysing α-particle spectra has been written in APL, which allows small peaks in a multiplet to be resolved simultaneously with large peaks. Al KX-ray fluorescence sources with emission rates from 10^3 to $10^5 s^{-1}$ were prepared and calibrated with a 3 % uncertainty.
In the field of metrology of neutron flux and dose CBNM reported to BIPM results on the usefulness of the two spheres-method at neutron energies of 2.5 and 14.8 MeV for neutron fluence determination. Two uranium-loaded parallel-multiplate fission chambers were built and tested for their timing properties (10 to 12 ns). They are to be used as transfer instruments for fast neutron fluence measurements. Neutron field and dose determinations were provided for neutron irradiations of mice for the Radiobiology Department of SCK/CEN Mol.

NUCLEAR DATA

NUCLEAR DATA FOR STANDARDS

Neutron Data for Standards

Fission Mode Fluctuations in Resonances of $^{235}U(n,f)$

H.-H. Knitter, F.-J. Hambsch*, R. Vogt

(WRENDA request nr. 781192R)

The evaluation of the raw experimental data was finalized during the preceding year. In the present reporting period the results were presented at the International Conference on Nuclear Data for Science and Technology in Mito, Japan, and a paper on this extensive work was elaborated for publication.

Fission fragment mass and total kinetic energy distributions were measured for single, isolated resonances and neutron energy bins covering the incident neutron energy range from 0.006 eV to 130 eV. The measurements were performed at the Geel Electron Linear Accelerator (GELINA) using a Frisch-gridded ionization chamber.

Fluctuations of the fission fragment mass distributions as function of resonance energy were observed, which are correlated with fluctuations of the reaction Q-value and with the measured total kinetic energy <TKE> averaged over all fragments. In the resonance region fluctuations in <TKE> from resonance to resonance are observed with amplitudes up to about 450 keV.

The correlations between the mass-distribution fluctuations and other parameters like spin J, spin orientation quantum number K, angular distribution fluctuations and the fluctuations of the average number of neutrons emitted in fission, $\bar{\nu}$, are evaluated and discussed. An interpretation of the $\bar{\nu}$-fluctuations observed in other experiments is given in terms of the mass distribution fluctuations. The fluctuations of the mass-distribution parameters and the total kinetic energy distributions as function of mass are viewed in the frame of the fission channel model of Bohr[1] and of the recent multi-fission mode random neck-rupture model of Brosa et al.[2].

---

* From October 1st, 1988

(1) A. Bohr, Proc. Intern. Conf. Peaceful Uses of Atomic Energy, UN, Geneva (1955), p. 151

(2) U. Brosa, S. Grossmann, A. Müller, Z. Naturforsch. 41a (1986) 1341

Investigation of the Spontaneous Fission of ^{252}Cf

H.-H. Knitter, U. Brosa*, R. Vogt
(Wrenda request nrs. 792189R, 821026R)

The aim of this experiment is to contribute to the basic understanding and to the improvement of the ^{252}Cf standard fission neutron spectrum. In these measurements on the spontaneous fission of ^{252}Cf, fission fragment parameters were determined simultaneously with those of the fission neutrons.

The evaluation of the experimental data has continued. However, a large part of the experimental information was already described in an extensive paper.

The gridded twin ionization chamber developed at CBNM is used to measure the kinetic energy, mass and angular distributions of the fission fragments of the spontaneous fission of ^{252}Cf. Together with a neutron time-of-flight detector this experimental arrangement permits to measure the correlations between neutron emission, fragment angle, mass and energy of the fission fragments. Without neutron coincidences $40 \cdot 10^6$ fission events were recorded which are evaluated to give mass, total kinetic energy and the variance distributions in a broad mass range from mass 67 to 185. About $3 \cdot 10^6$ fission events were recorded in coincidence with a neutron detected in the time-of-flight detector. Angular distributions in the center-of-mass (CM) system revealed isotropy in the whole fission neutron energy range. This permits the conclusion that fission neutrons are emitted from the fully accelerated fragments and that the hitherto assumed scission neutron component of 15-20 % is much smaller, as can be determined from the uncertainty of the second Legendre polynomial coefficient. The average number of neutrons was determined as function of fragment mass and TKE. The mass range for $\bar{\nu}(A)$ was extended beyond that of earlier measurements and revealed two new "sawteeth" near masses 80 and 176. The slopes and end points of $\bar{\nu}(TKE)$ were also determined for each fragment mass. The fragment CM fission neutron spectra were determined as function of fragment mass and TKE. These spectra permitted the evaluation of the average neutron energy $\bar{\eta}(A,TKE)$, the nuclear temperature $T(A,TKE)$ and the λ-factor from the cascade evaporation model. These quantities permitted the evaluation of the level density parameter $a(A)$ in the mass range from 90 to 169.

---

* Scientific Visitor from Philipps University of Marburg, Germany

The ^{252}Cf experiment gave the following important results:

(1) The fission neutron angular distributions in the angular range between 0° and 90° in the fission fragment centre-of-mass system could be determined as function of neutron energy without disturbance from neutrons of the complementary fragment. The limitation of the above mentioned angular range means that only events with neutron energies in the laboratory system larger or equal than the fragment energy per nucleon are included in the evaluation.

(2) The angular distributions in the ranges for the CM neutron energies (0-10 MeV) and the CM angles (0-90 degrees) were found to be isotropic.

(3) For each fission fragment mass and each fragment total kinetic energy bin of ~2 MeV a fission neutron spectrum in the fragment CM system was evaluated and analysed in the frame of the cascade evaporation model with the functional relationship:

$$\phi\ (\eta) = \text{const}\cdot\ \eta^{\lambda}\cdot e^{-\eta/T}$$

with η the neutron energy in the fragment CM system. This analysis results in two data sets for the parameters λ(A,TKE) and T(A,TKE) describing the neutron spectra in the fragment CM system.

(4) The experimental fragment yield as function of fragment mass and total kinetic energy measured in coincidence with those neutrons as discribed in point (1), Y_{CO}(A,TKE), together with the data sets T(A,TKE) and λ(A,TKE), permitted, under the assumption that the angular distributions of the neutrons in the CM system were symmetric with respect to 90°, the calculation of the fission neutron spectrum in the laboratory system also at very low neutron energies.

(5) The transformation calculations to the laboratory reference system showed that the low energy part of the fission neutron spectrum is mainly determined by the velocity distribution of the fission fragments and is only little dependent on other parameters. Fig.1 shows the calculations with the measured data λ(A,TKE), λ=0.5, a value often used in cascade evaporation theory, and λ(A) which is the value averaged over all TKE-values.

Little variations are observed for the calculated low energy part of the laboratory fission neutron spectrum. The full points in Fig.1 are those from the evaluation of direct measurements made by Mannhart[1].

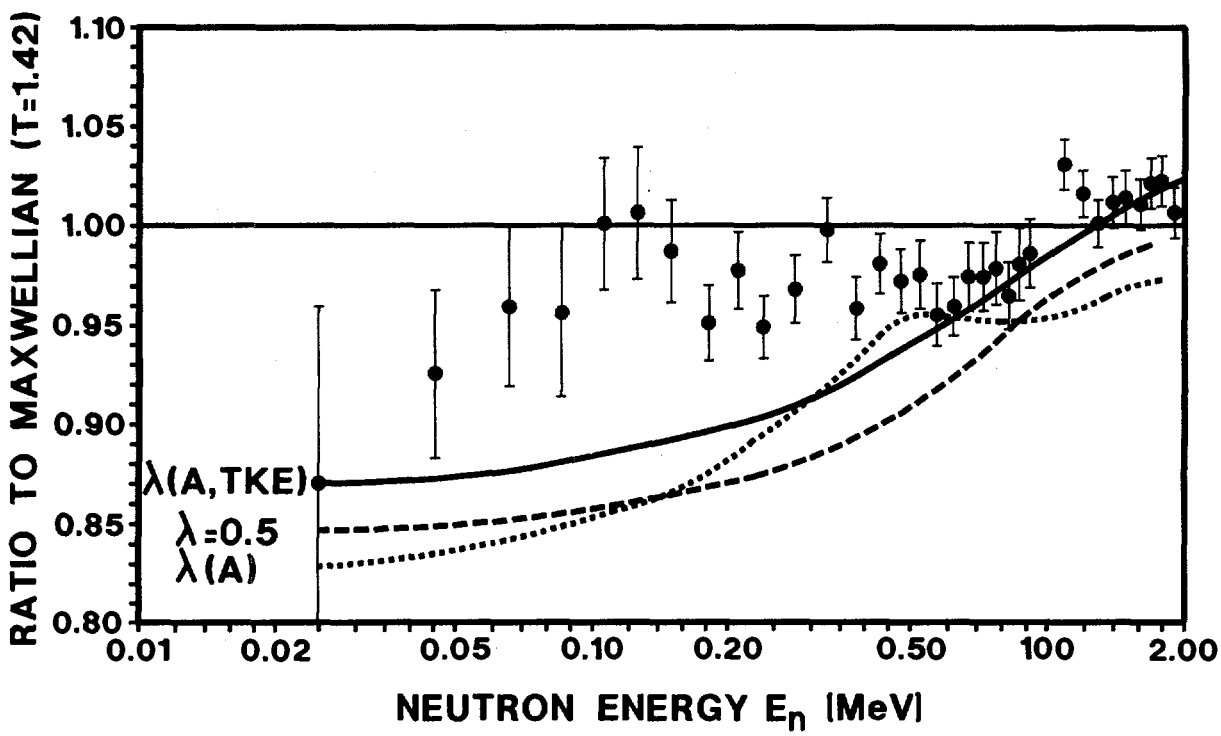

Fig. 1. Low energy part of the laboratory fission neutron spectrum ^{252}Cf. The spectrum is plotted as a ratio with respect to a Maxwellian with T = 1.42 MeV. Full points are from the evaluation of Mannhart [1]. The lines are from transformation calculations using different data for λ

The difference between the evaluation of Mannhart[1] and the present transformation calculations can be an experimental artefact caused by imperfections of earlier experiments or a contribution from a particular low energy neutron source. If the second assumption is considered then a scission neutron spectrum is obtained as shown in Fig.2.

The average energy of these neutrons is (0.39 ± 0.06) MeV and their fraction of all prompt neutrons is (1.1 ± 0.3) %. The low energy of these scission neutrons suggests a production mechanism analog to the process responsible for the satellite droplet production in the desintegration of liquid jets. They are just born without major kinetic energy in between the fragments. Their energy distribution is determined

(1) W. Mannhart, Evaluation of the ^{252}Cf Fission Neutron Spectrum, Proc. of an IAEA Advisory Meeting, Leningrad 1986, IAEA-TECDOC-410, IAEA Vienna 1987, p.158

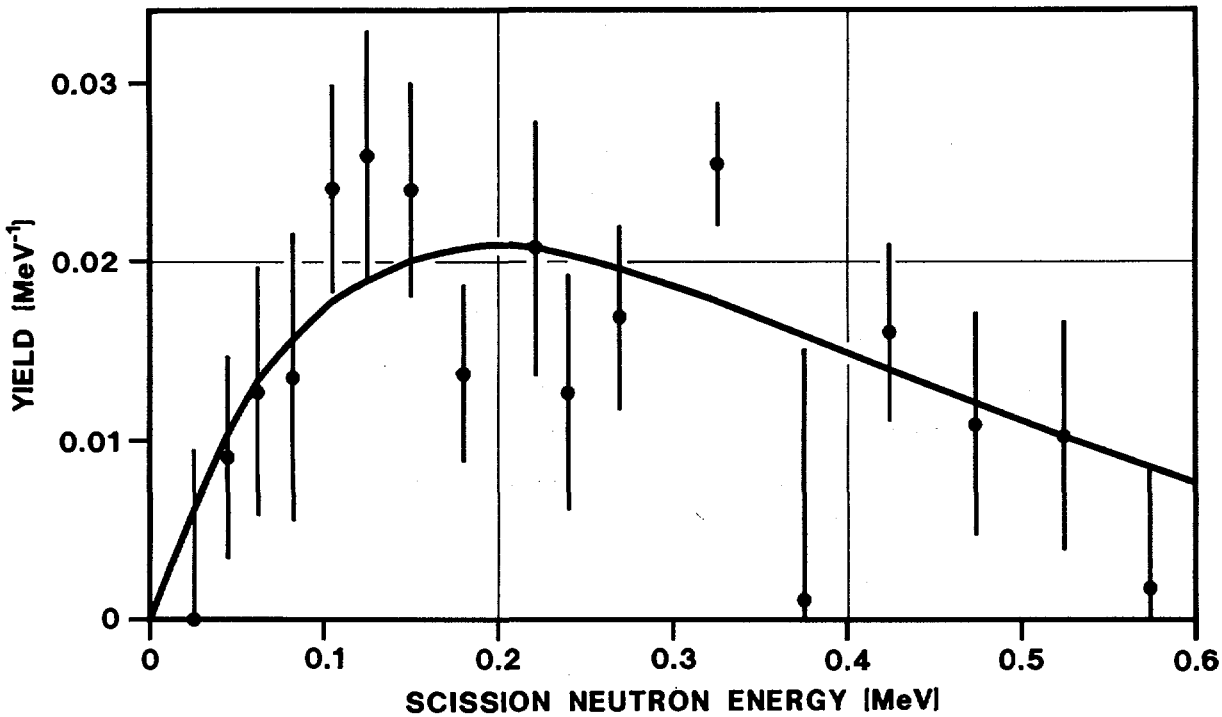

Fig.2. Scission neutron spectrum obtained as a difference between the transformation calculation and the evaluated points as shown in Fig.1. The full line is a fit with a Weisskopf distribution through the above points yielding the average neutron energy and the partition of the scission neutrons as given in the text

by Heisenbergs uncertainty relation and the dimensions of the neck-region of the prescission shape. This is the first time that the spectrum shape and the fraction of the scission neutrons can be given.

Non-Neutron Nuclear Data for Standards

Half Life of ^{125}I

T. Altzitzoglou

During the meeting of the IAEA Coordinated Research Programme on the Measurement and Evaluation of X- and Gamma-Ray Standards for Detector Calibration in Rome, 11 to 13 June 1987, more accurate measurements of the half life of ^{125}I were recommended as a first priority item[1]. Half-life uncertainties influence considerably the accuracy of the calculated standard

---

(1) P. Christmas, A.L. Nichols, A. Lorenz, INDC (NDS)-/96/GE (1987)

source activity after a period of several half lives. Uncertainties of better than 0.03 % are considered necessary [1].

Several ^{125}I sources were prepared and sealed in Al containers (diameter 15 mm, thickness 1.5 mm). They were counted regularly using both a 76 x 76 mm NaI(Tl) and a Ge(Li) detector. The NaI(Tl) system has the advantage of high stability over long periods, but the method is sensitive to impurities in the source. The semiconductor system has no such problem due to its high resolution. The long-term stability of the detectors and the associated electronics is checked using long-lived radionuclides.

The evaluation of the measured data is performed by regression analysis. To avoid systematic effects the data were divided into subgroups in various patterns. This facilitates the realistic estimation of an uncertainty.

Measurements were performed in 3 different geometries over about one half life. Approximately 330 spectra were measured with the Ge(Li) detector. The analysis of these data is in progress. A total of 275 data points taken with the NaI(Tl) detector were analysed. No impurities were detected. The results agree well with each other.

Alpha Particle Emission Probabilities, P_α, of ^{237}Np

G. Bortels, D. Mouchel

Re-analysis of the spectra which had been used previously for the P_α measurements of ^{237}Np resulted in the determination of two more weak peaks; one at 4619 keV with P_α = 0.0005 and the other at 4748 keV with P_α = 0.0012.

In a spectrum from a mixed ^{237}Np + ^{240}Pu source the (5168.17 ± 0.15) keV peak of ^{240}Pu was used as an internal energy reference to measure the energies of the ^{237}Np peaks. Peak positions were analyzed with a precision (standard deviation) of typically better than 0.1 keV. However, the energy of the major peaks in the ^{237}Np decay obtained in the calibration turned out to be too high by about 1.5 keV. This deviation could be due to pulser non linearity and/or to unsatisfactory corrections of the pulse-height defect for alpha particles in silicon. Alpha-particle energies used in the calibration were corrected for electronic losses outside the detector volume and for atomic losses in the detector which do not contribute to

(1) K. F. Walz, K. Debertin, H. Schrader, Int. J. Appl. Radiat. Isot. 34, (1983) 1191; H. Schrader, PTB Progress Report GS/38 (1988) for the IAEA CRP

the creation of electron-hole pairs. The alpha particles loose about 1.7 keV in the NpO_2 layer which has a thickness of about 6.1 $\mu g/cm^2$ as calculated from the activity and source diameter. Further energy loss of 5.5 keV occurs in the detector entrance window. Losses due to elastic collisions in the silicon lattice are not very well known but estimates from the work of Lennard and Winterbon[1] led to a value around 10.8 keV. For electronic losses the energy dependence is quite well known. For atomic losses, however, available data are not accurate enough. Adopting an energy of 4788.1 keV for the major peak in the ^{237}Np decay a non-linearity correction was made enabling to assess the remaining alpha-particle energies. The non-linearity problem requires further investigation.

---

(1) W. N. Lennard, K. B. Winterbon, Nucl. Instrum. Meth. Phys. Res. B24/25 (1987) 1035

NUCLEAR DATA FOR FISSION TECHNOLOGY

Neutron Data of Actinides

A discrepancy is known to exist between the calculated temperature coefficient of reactivity for light water reactors and measured values obtained in integral experiments[1]. This discrepancy is of the order of 3 to 5 pcm/°C, while the commonly accepted goal for the accuracy of this parameter is 1 pcm/°C. In order to account for this effect, Santamarina et al.[2] have proposed that the energy dependence of certain differential nuclear data in the sub-thermal neutron energy region be modified with respect to the evaluated Data File ENDF/B-5 within their experimental uncertainties. The quantities concerned are the fission cross section, σ_f, and the number of fission neutrons emitted per neutron absorbed, η, of ^{235}U, as well as the capture cross section, σ_γ, of ^{238}U.
Following a suggestion of French and British reactor physicists, a complete measurement program of these quantities has been started at GELINA in 1985; to this end a liquid methane moderator kept at 110 °K temperature has been installed around the neutron producing target, yielding about five times more neutrons below 20 meV as compared to the usual room temperature water moderator. Results are given in the following, separately for three different measurements. While the fission data for ^{235}U, as well as for ^{233}U and ^{239}Pu, and the capture data for ^{238}U have been published recently and can be considered as final, difficulties still subsist for η of ^{235}U.
Additional effort went to the studies made on $^{235}U(n,f)$ with very cold neutron and on the spontaneous fission of plutonium isotopes.

Fission of ^{233}U, ^{235}U and ^{239}Pu

C. Wagemans*, P. Schillebeeckx**, A.J. Deruytter, R. Barthélémy

These investigations were extended to the other common fissile nuclei ^{233}U and ^{239}Pu since the σ_f data base in the subthermal energy region appeared also rather poor for them.

---

* SCK/CEN, Mol and R.U. Gent, Belgium
** Scientific Visitor now at ILL, Grenoble, France
(1) J. Bouchard, C. Golinelli, H. Tellier, Nuclear Data for Science and Technology, Reidel Publ. Comp. (1983), p. 21
(2) A. Santamarina, C. Golinelli, L. Erradi : ANS Topical Meeting on Advances in Reactor Physics, Chicago (1984)

The measurements were performed at a well collimated 8.2 m flight-path of GELINA. The accelerator was operated at a 40 Hz repetition frequency with 2 μs burst width and with an average electron current of 15 μA. An evaporated layer of 25 μg $^{6}LiF/cm^{2}$ for the neutron flux determination and a fissile layer were mounted back-to-back in the centre of a vacuum chamber with 50 cm diameter. The particles and the fission fragments from the reaction $^{6}Li(n,\alpha)t$ were detected in a low geometry with two 20 cm^{2} large surface barrier detectors placed outside the neutron beam.
The thicknesses of the layers were chosen in such a way that absorption and self-absorption effects were very small. Homogeneously evaporated fluoride layers with the following thicknesses were used: 40 μg $^{233}U/cm^{2}$; 40 μg $^{235}U/cm^{2}$ and 30 μg $^{239}Pu/cm^{2}$.
The neutron energy scale in the meV region was verified by means of the prominent Bragg-reflection cuts in Be at 5.24 and 6.84 meV. The background was determined using the black resonances of cadmium, rhenium, gold and tungsten. The background due to neutrons from overlapping bursts was checked by operating GELINA at 20 Hz. In Fig. 3 the total $^{235}U(n,f)$ and $^{6}Li(n,\alpha)t$ counting-rate spectra are shown with the corresponding normalized background curves (lower full lines).

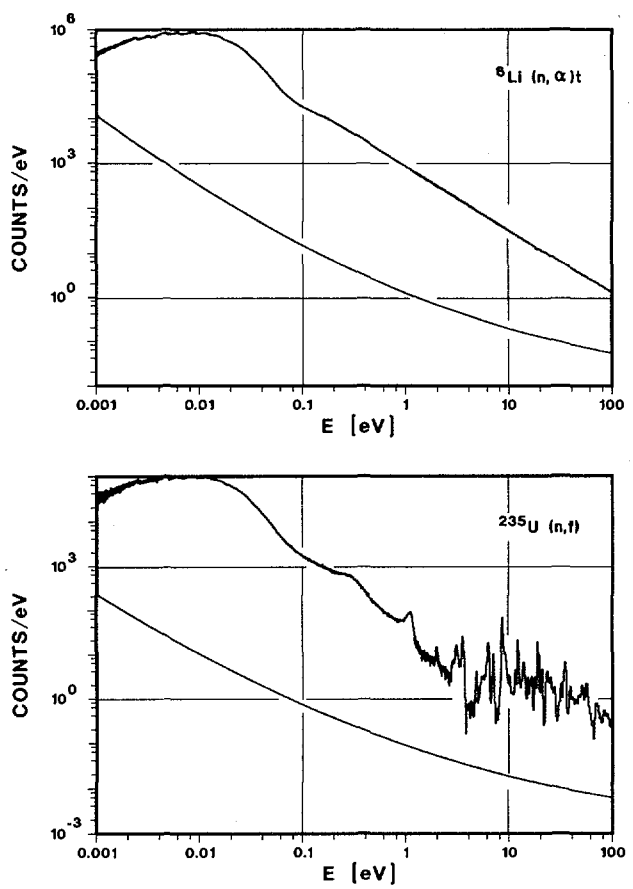

Fig.3. $^{6}Li(n,\alpha)$ and $^{235}U(n,f)$ counting-rate spectra with the corresponding normalized background curves (lower full lines)

All fission measurements were performed relative to the $^{6}Li(n,\alpha)t$ reaction, for which a 1/v shape was assumed in the energy region below 20 eV. The data reduction was done at the IBM 4381 using the APL language and the ANGELA routine.
The ratio of the background corrected fission and (α+t) counting-rates yields the $\sigma_f(E)\sqrt{E}$ shape, which still needs to be normalized. This normalization was done in the thermal region relative to the $\sigma_f°$ values proposed for the ENDF/B-6 file, i.e.: 531.14 b (± 0.25 %) for ^{233}U, 584.25 b (±

0.19 %) for ^{235}U and 748.0 b (± 0.25%) for ^{239}Pu, via selected fission integrals. This normalization procedure was cross-checked by a polynomial fit through the normalized $\sigma_f(E)\sqrt{E}$ data in the thermal region, yielding consistent $\sigma_f°$-values.

Fig.4 shows the measured $\sigma_f(E)\sqrt{E}$ data for ^{235}U (histogram) in the neutron energy range from 2 meV to 1 eV. The full line is the ENDF/B-V curve (renormalized to $\sigma_f°$= 584.25 b). The experimental data and the evaluated file agree within the errors above thermal energy. Below this energy, an agreement exists within two standard deviations although the measured data below 10 meV clearly go faster to a 1/v-shape than the evaluated curve.

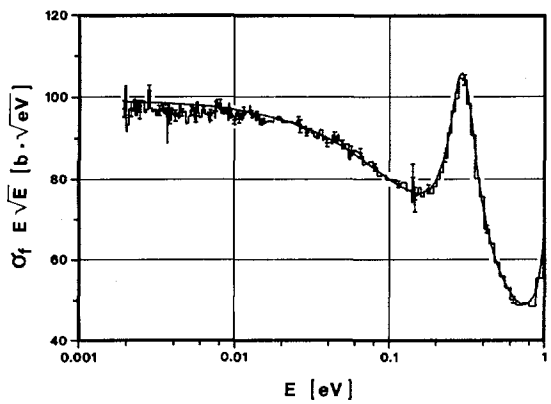

Fig.4. Measured $\sigma_f(E)\sqrt{E}$-histogram for ^{235}U. The full line is the ENDF curve renormalized to $\sigma_f°$ = 584.25 b

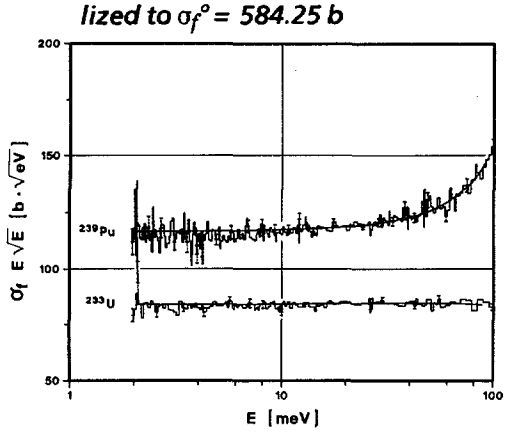

Fig.5. Measured $\sigma_f(E)\sqrt{E}$-histogram for ^{233}U and ^{239}Pu. The full lines are the renormalized ENDF curves

Fig. 5 shows the ^{233}U $\sigma_f(E)\sqrt{E}$-data in the neutron energy region from 2 meV to 100 meV together with the corresponding results for ^{239}Pu. Also the present ^{239}Pu data agree with the ENDF/B-4 curve within the experimental uncertainties, although they tend to be slightly lower below 10 meV. Since these σ_f measurements were performed under excellent measuring conditions (low repetition frequency, low background, thin samples), they were also used to calculate selected fission integrals. There is a good agreement between the present results and those of Gwin et al.[1] for ^{235}U and ^{239}Pu. Also the renormalized ENDF/B-5 values are in fair agreement. New calculations of Westcott g_f factors were done for ^{233}U, ^{235}U and ^{239}Pu, making only use of the present fission data.

The extrapolation towards zero energy was done by using a least squares fit $\sigma_f\sqrt{E} = a+bE+cE^2$ which was applied to the data points in the energy region from 2 meV to 100 meV. This extrapolated part contributes only with about 1.5% to the g_f value at T = 20.44 °C. The $g_f(T)$ curves obtained in this way are shown in Fig. 6. The values at T = 20.44 °C are given in Table 1, which includes a series of evaluated values.

---

(1) R. Gwin, R.R. Spencer, R.W. Ingle, J.H. Todd, S.W. Scoles, Nucl. Sci. Eng. 88 (1984) 37

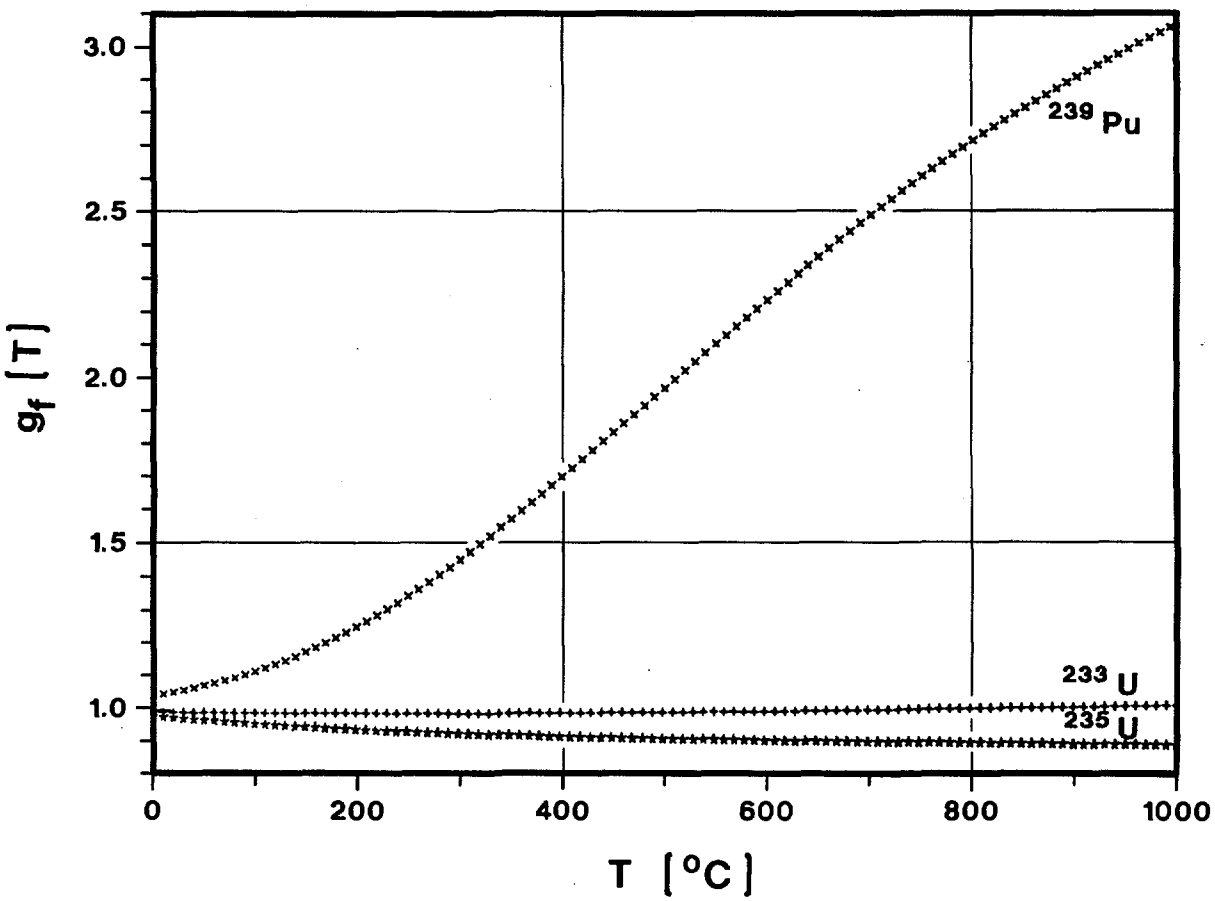

Fig.6. $g_f(T)$ curves calculated from the present $\sigma_f(E)$ data

Table 1. Westcott g_f-factors at T = 20.44 °C

Reference	^{233}U	^{235}U	^{239}Pu
Hanna (1969)	0.9950 ± 0.0021	0.9766 0.0016	1.0548 ± 0.0030
Steen (1972)	0.9966	-	-
Leonard (76/81)		0.9775 ± 0.0011	1.0535 ± 0.0015
Lemmel (75/82)	0.9967 ± 0.0017	0.9762 ± 0.0012	1.0555 ± 0.0024
Divadeenam (1984)	0.9955 ± 0.0015	0.9761 ± 0.0012	1.0558 ± 0.0023
Axton (1986)	0.9955 ± 0.0014	0.9774 ± 0.0008	1.0555 ± 0.0022
ENDF/B-5	0.9966	0.9775	1.0582
ENDF/B-6	0.9955 ± 0.0014	0.9771 ± 0.0008	1.0563 ± 0.0021
Present work	0.994 ± 0.003	0.976 ± 0 002	1.055 ± 0.003

Eta of ^{235}U

B. Keck*, J.A. Wartena, H. Weigmann, C. Bürkholz, P. Geltenbort**, K. Schreckenbach**

A first measurement campaign has been performed at the GELINA pulsed white neutron source. The data indeed indicate that the energy dependence of η may deviate from the constant assumed in ENDF/B-5 in the sub-thermal region by up to 2 %. However, these data are considered only as a preliminary indication, because the measurements suffered from background problems which are difficult to control. Therefore, a new experiment has been set up at a neutron beam of the ILL high flux reactor, with the conditions being improved as compared to the linac measurement in two ways: the neutron spectrum is much more suited, with less high energy neutrons which in the time-of-flight experiment are the source of the background problems at lower energies (longer flight times); by the installation of two choppers essentially a pulsed monoenergetic beam is produced, and background events in the detectors due to scattered neutrons are separated in time from true events. The two choppers are running asynchronuously, hence the energy of the neutron beam is continuously varied, the phase between the two choppers being registered with each detector event.

The neutron beam emerging from the two choppers first passes a flux monitor (an ionization chamber loaded with a 154 $\mu g/cm^2$ $^{235}UF_4$ sample). About 90 cm downstream the beam hits a metallic ^{235}U sample which is sufficiently thick to absorb all neutrons with energies of interest.

Fission neutrons emerging from this sample are detected by a NE 213 liquid scintillator detector with pulse shape discrimination to distinguish fission neutrons from γ rays. The shape of the neutron flux at the position of the thick uranium sample is measured in separate runs by replacing the uranium sample by either a ^{10}B or a cadmium sample, and recording the emitted γ rays. Since also these samples are sufficiently thick that all neutrons with energies of interest are captured, the shape of the neutron flux is directly obtained from the measured γ ray yield. The ionization chamber mentioned above only serves to record any possible changes in the neutron flux shape between the different runs. After some preliminary measurements done in early 1988, a definite measurement campaign was performed in October. The analysis of the data is in progress.

---

* Scientific Visitor from TH Darmstadt, Germany

** ILL, Grenoble, France

Capture of ^{238}U

F. Corvi, G. Fioni*

The measurements were performed at a 8.68 m flight path at GELINA operated with the same parameters as for the fission runs. The sample, surrounded by a 0.6 cm thick ^{6}Li sleeve, was contained in an evacuated aluminium pipe: it consisted of a thin plate of highly depleted (99.999 % ^{238}U) uranium metal of size 6x6 cm and weight 13.8 g, whose thickness was equivalent to N = $9.68 \cdot 10^{-4}$ at/b. It was viewed by four C_6D_6 liquid scintillators of 10.2 cm diameter and 7.6 cm height, housed in a large shielding facility with walls made of 14 cm thick lead and 25 cm thick borated wax. The time-dependent background was measured by replacing the sample with an equivalent graphite scatterer. The neutron flux at the position of the uranium sample was measured in a separate run by replacing the ^{238}U with a sintered B_4C disk of 0.06 cm thickness and 8 cm diameter, enriched to 93 % ^{10}B. The 478 keV γ rays from the reaction $^{10}B(n,\alpha\gamma)$ were detected with the same C_6D_6 scintillators. The constancy of the flux during the various runs was checked by a double gridded ionization chamber placed in the beam before the shielding and loaded with back-to-back deposits of ^{10}B of 5 $\mu g/cm^2$ thickness. The signal-to-background ratio of the capture run was improved by a factor 5, by counting only coincidences between γ rays depositing more than 0.15 MeV in any two detectors. In this way it was possible to achieve a ratio of 16:1 between the peak counting rate per time-of-flight unit, obtained at about 25 meV, and that at 0.8 meV neutron energy where the flat background was mainly due to sample activity.

In order to check that the coincidence rate well represents the actual capture rate, a run in the resonance region was performed in which the number of coincidences C was compared to that of weighted singles S for twenty-two s-wave resonances in the range from 6 to 478 eV. It was found that the relative standard deviation of the C/S population was 2.7 % and that all values were included in the interval spanning ± 6 % from the average. In the present thermal capture case, the only variation with neutron energy of the γ spectrum can be due to the E_0 = -0.005 eV resonance postulated by Santamarina et al.[1] whose relative contribution varies from about 1 % at 0.100 eV to 41 % at 0.002 eV.

---

* EC fellow

(1) A. Santamarina, C. Golinelli, L. Erradi : ANS Topical Meeting on Advances in Reactor Physics, Chicago (1984)

Therefore the maximum systematic error associated with the coincidence measurement is $\varepsilon = 0.4 \times 6\ \% = 2.4\ \%$. This error has been considered over the whole energy range.

In a second measurement campaign the metallic sample was replaced by a 59.8 g sample of U_3O_8, of thickness $N = 2.56 \cdot 10^{-3}$ atoms $^{238}U/b$, also depleted to 99.999 % and canned in a thin wall aluminium container of 8 cm diameter. This material was measured immediately after having been chemically purified so that the amount of radioactive decay products was strongly reduced with respect to the secular equilibrium case. This reduction in activity was however partly compensated by an increase of the energy dependent background mainly due to neutron capture in the container. As a consequence, the peak-to-background ratio defined previously reached a value of 22:1. Both samples were chemically pure to about 99.9 %: amongst the several impurities detected by spark source mass spectrometry none contributed an appreciable fraction to the thermal neutron capture in the sample. Two types of background were considered and separately subtracted: the first one was a time-dependent background, measured by replacing the ^{238}U sample by an equivalent graphite scatterer. The second was the background associated with the activity of the ^{238}U sample and assumed constant with time-of-flight. It was measured during the main capture runs in the energy interval 0.65-0.78 meV, where the neutron flux was negligible.

The measured values of $\sigma_\gamma \sqrt{E}$ for ^{238}U are given in Fig. 7 for the metal and for the oxide sample, respectively, and compared with the predictions of the available evaluations. Since the goal here is to compare only the shapes of experimental and calculated curves and not the absolute values, it is convenient to make all curves coincide at the upper energy end so that one can look how much the data diverge (or converge) on the low energy side. In absolute terms this is not exact because the two evaluations are normalized to the same value $\sigma_\gamma = 2.70$ b of the 2200 m/s cross section. To take that into account, the JEF-1 curve is referred to the left hand vertical scale and the Santamarina[1] evaluation to the right hand one. The JEF-1 curve (full line) is in fact representative of any evaluation which does not foresee a negative energy resonance in the immediate vicinity of zero energy. It has practically a 1/v behaviour except for a 1 % slope in the considered energy range due to the influence of the 6.67 eV resonance. The surmise of Santamarina et al.[1] on the contrary exhibits a very different slope.

---

(1) A. Santamarina, C. Golinelli, L. Erradi : ANS Topical Meeting on Advances in Reactor Physics, Chicago (1984)

An inspection of posts (a) and (b) of Fig. 7 shows that, for both samples, the experimental points disagree with this last evaluation but agree within the errors with the JEF-1 curve. Therefore the assumption of a resonance at E_0 = -0.005 eV should be dropped.

To conclude, the results of the present experiment confirm the approximate 1/v dependence of the ^{238}U thermal capture cross section foreseen by most evaluations. As a consequence, the possibility of explaining the experimental values of the temperature coefficients of reactivity with a different slope of this cross section should be ruled out.

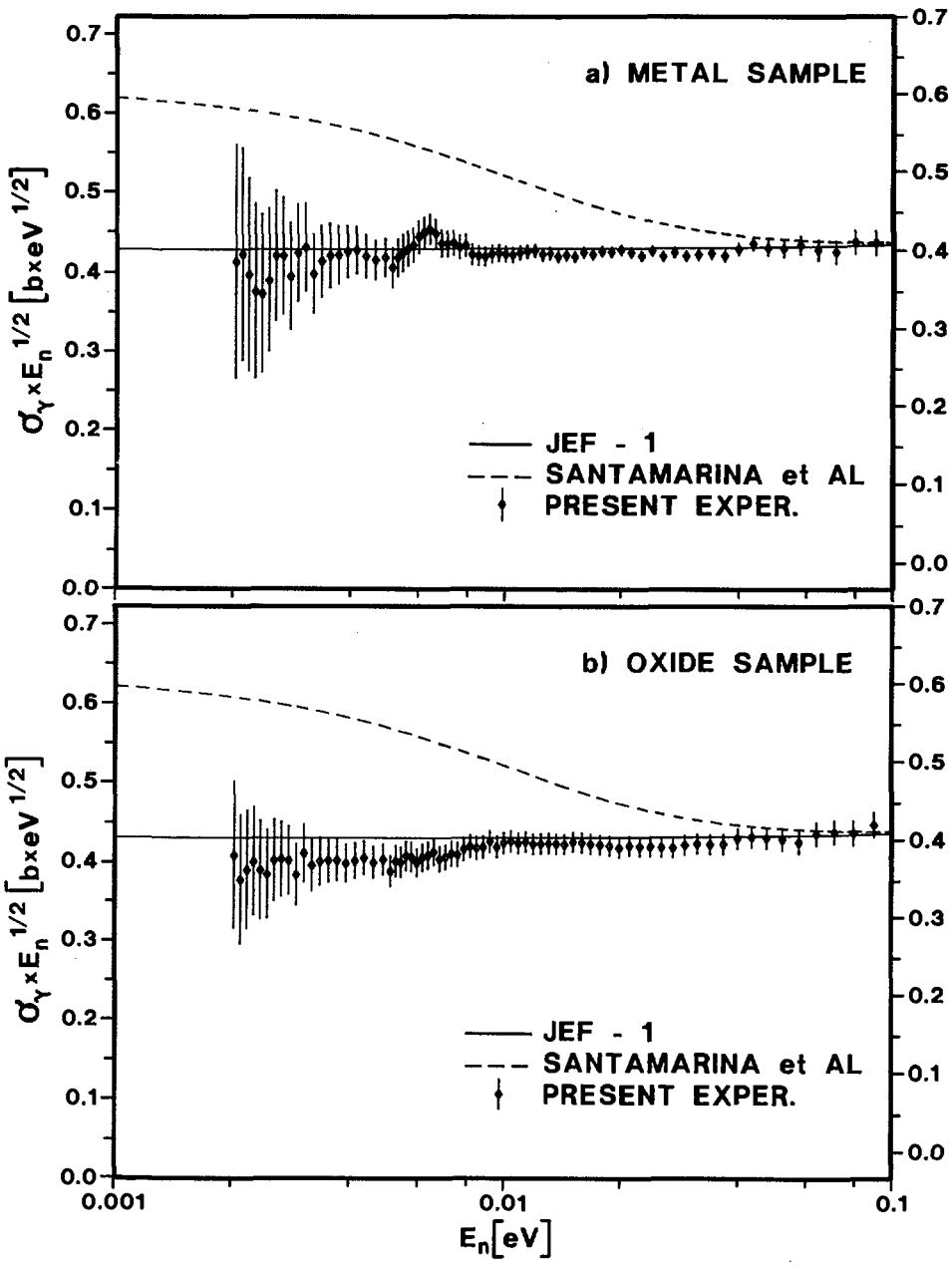

Fig. 7. Experimental points of $\sigma_\gamma\sqrt{E}$ of ^{238}U plotted vs energy and compared to the JEF-1 and Santamarina evaluation for : a) the metal sample; b) the oxide sample. All data sets are normalized to the same value at the upper energy end.

Investigation of the Shape of the $^{235}U(n,f)$ Cross Section with Very Cold Neutrons

C. Wagemans*, A.J. Deruytter, R. Barthélémy, W. Mampe**, P. Ageron**, A. Michaudon**

At the very cold neutron source of the ILL Grenoble, the shape of the $^{235}U(n,f)$ cross-section has been measured in the μeV-neutron energy region. For this purpose, a slow chopper has been installed at the end of the very cold neutron guide. Very thin $^{235}UF_4$ and ^{6}LiF samples and PIPS detectors were used for the detection of the $^{235}U(n,f)$ fragments and for the determination of the neutron flux via the $^{6}Li(n,\alpha)t$ reaction. Within the experimental accuracy, the present results do not show a significant deviation of the $^{235}U(n,f)$ cross section from a 1/v shape.

Investigation of Neutron Shell Effects and Fission Channels in the Spontaneous Fission of the Plutonium Isotopes

P. Schillebeeckx***, C. Wagemans*, A.J. Deruytter, R. Barthélémy

The energy and mass distributions of the spontaneously fissioning plutonium isotopes are a crucial test for the finesse of fission theories. These characteristics for $^{236,238,240,242,244}Pu$ form an ideal data base for the study of shell effects and fission channels under identical conditions. Indeed, all these isotopes have Z = 94, $I^{\pi} = 0^{+}$ and zero excitation energy, the only difference being the number of neutrons. The strong impact of the neutron number on the fission fragment mass distribution is illustrated in Fig. 8, which shows the experimental and fitted three-dimensional spectra for the heavy fragments' peak in $^{238,240,242}Pu$(s.f.). The presence of two fission modes (one centred around mass 135, the other centred around mass 142) with strongly varying importance is clearly demonstrated. Fig. 9 displays the corresponding mass distribution of the heavy fragments, completed with results which were recently obtained for ^{236}Pu(s.f.). Both figures clearly show that, when going form ^{236}Pu to ^{242}Pu, the yield in the mass region around 142 decreases by more than a factor of two, which is compensated by an equal increase of the yield in the mass region around 135. The average total fission fragment kinetic energy on the other hand systematically decreases when going from ^{244}Pu to ^{236}Pu, instead of the expected increase with increasing values of $Z^2/A^{1/3}$.

---

* NFWO, SCK/CEN, Mol and R.U. Gent, Belgium
** ILL, Grenoble, France
*** Scientific Visitor from R.U. Gent, Belgium

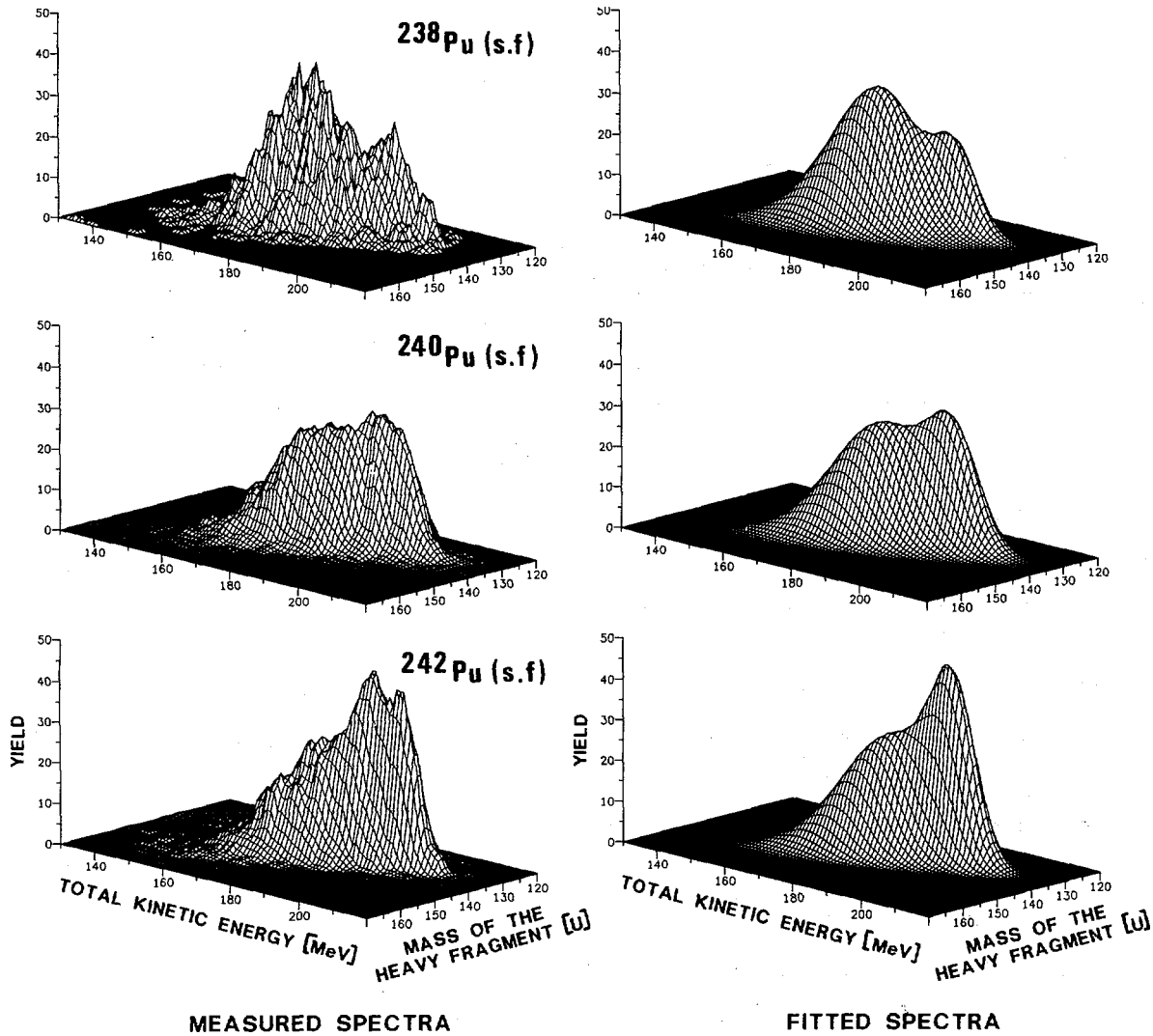

Fig.8. Three-dimensional distributions for the heavy fragments' peak in $^{238,240,242}Pu$ (s.f.)

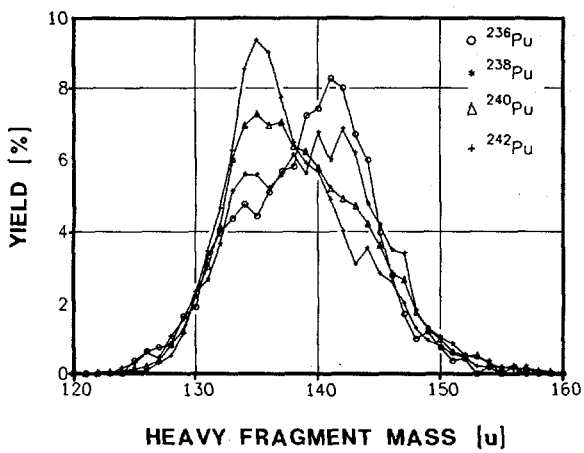

Fig. 9. Heavy fragment mass distribution for $^{236,238,240,242}Pu$(s.f.)

These results can be explained and even quantitatively reproduced in a satisfactory way in terms of the fission channel model of Brosa et al[1]. This is illustrated in Table 2, in which calculated parameters of the Standard I and Standard II fission channels in ^{240}Pu(s.f.)[2] are compared with the corresponding experimental values deduced from Fig. 8. Only the calculated width of the Standard II mass distribution is significantly smaller than the experimental value, which might be due

to the adoption of a too low intrinsic temperature at the scission point and/or the neglection of the width of the potential energy surface in the mass-asymmetric direction.

Table 2. Calculated [2] and experimental parameters of the Standard I (St I) and Standard II (St II) fission channels in ^{240}Pu(s.f.)

Parameter		Calculated St I	Calculated St II	Experimental St I	Experimental St II
$\bar{m}_h^*$	[u]	135	139	134.4	140.1
$\sigma_{\bar{m}_h}^*$	[u]	2.4	4.1	2.8	5.7
$\bar{E}_k^*$	[meV]	192	172	192.2	174.8

Furthermore, the relative position of the potential energy curves in Fig. 10 explains the measured relative peak yields shown in Figs. 8-9. This fair agreement between experiment and theory supports the idea of random neck-rupture as well as the calculated final configurations of the St I and St II channels.

These St I and St II fission channels can be associated with the closed and deformed fragment shells N = 82 and N ≈ 87 obtained in the scission point models[3,4]. The interplay of these shells with minor shells in the light fragment qualitatively explains the observed structures in the mass distribution of ^{238,240,242}Pu. It fails however in explaining the strong enhancement of the yield in the mass region of 142 experimentally obtained for ^{236}Pu. This might be due to the rather large uncertainty on the position of these minor shells. Another weak point of the scission point model calculations is the overestimation of the influence of the spherical shell N = 82, which results in too low average masses (for ^{240}Pu e.g. the calculated value of $\bar{m}_h^*$ is 132.3 contrary to an experimental value of 138.7) and in too small widths of the distributions.

(1) U. Brosa, S. Grossmann, Z. Phys. A310 (1983) 177,

(2) U. Brosa, S. Grossmann, A. Müller, to be published,

(3) B. Wilkins, E. Steinberg, R. Chasman, Phys. Rev. C14 (1976) 1832

(4) J. Moreau, J. Ryckebusch, K. Heyde, M. Warocquier, Proc. Journées d'Etudes sur la Fission, Arcachon, Report CENBG 8722, CEN Gradignan, France, 1987, p.C1

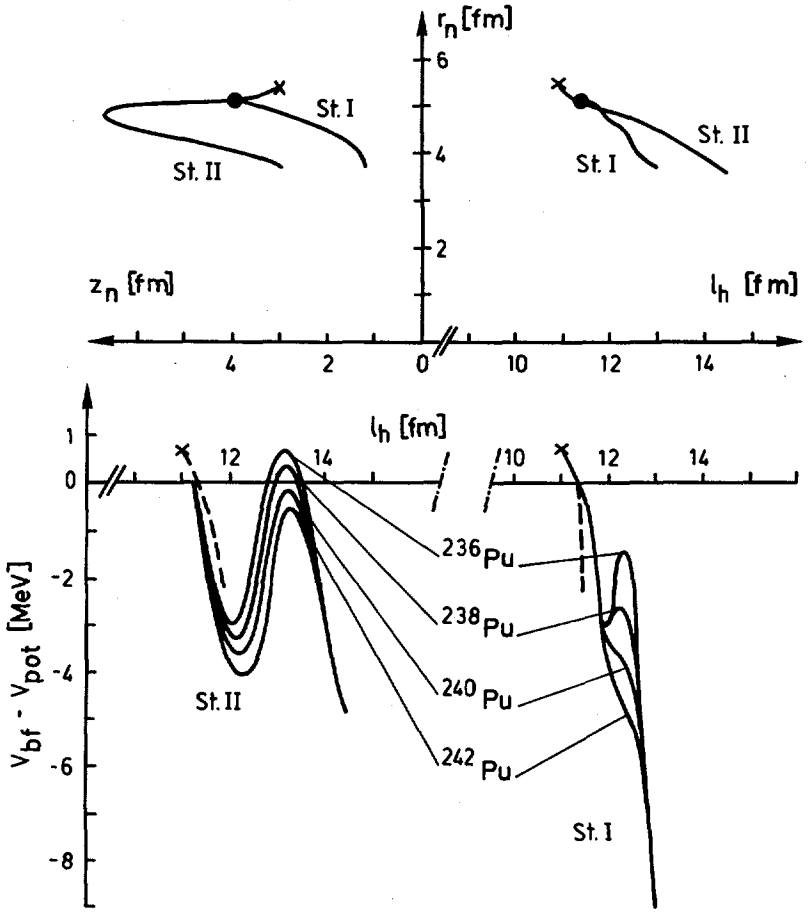

Fig. 10. *Upper part : standard I and standard II fission channels (projection of the valleys in the (r_n, z_n) and (r_n, l_h)-planes for ^{236,238,240,242}Pu(s.f.)*
Lower part : potential energy of both fission channels relative to that of the bifurcation point (.) between standard I and standard II [1]

Neutron Data of Structural Materials

The ^{56}Fe 1.15 keV Resonance Task Force

F. Corvi, G. Fioni*, F. Gasperini, P.B. Smith**

An invited paper with the title "Matters related to the NEANDC Task Force on ^{238}U and ^{56}Fe Resonances" has been presented in collaboration with M.G. Sowerby at the Int. Conf. on Nuclear Data for Science and Technology, Mito, May-June, 1988.

---

* EC Fellow
** Rijksuniversiteit Groningen, The Netherlands

The success of the experimental method of weighting function determination in reproducing the 1.15 keV resonance parameters obtained from transmission, and the large discrepancy between the experimental and the calculated response functions have stimulated a new series of calculations. In particular, F. Perey of ORNL has carried out a series of simulations of the (p,γ) experiment using the electron gamma transport code EGS from Stanford Linear Accelerator. The main improvements of this widely used code over the old ones are a correct treatment of the electron transport and the possibility of studying in a detailed way the influence of any material surrounding the source-to-detector configuration. The EGS code has met with a considerable success in calculating high-energy response functions which are much more similar to the experimental ones than the results of the old calculations. The agreement is however not yet satisfactory since the low pulse height region of the response functions (with the exception of the part below 0.5 MeV) is still 15 to 20 % lower than the experimental data. This situation is reflected in Fig. 11 where the absolute efficiency is plotted versus energy also for the EGS results (dash-and-dot line): one can notice that these data are in fact intermediate between the experiment and the previous calculations. Also, F. Perey has calculated response functions and efficiencies for the Geel neutron capture setup and found that these quantities are strongly dependent on sample thickness. He has in fact calculated a weighting function for each thickness of interest: the one corresponding to the 0.5 mm thick iron sample used in the normalization to silver and gold capture is also plotted in Fig. 12. Here again it can be seen that the W-function based on EGS is intermediate between the experiment and the old calculations.

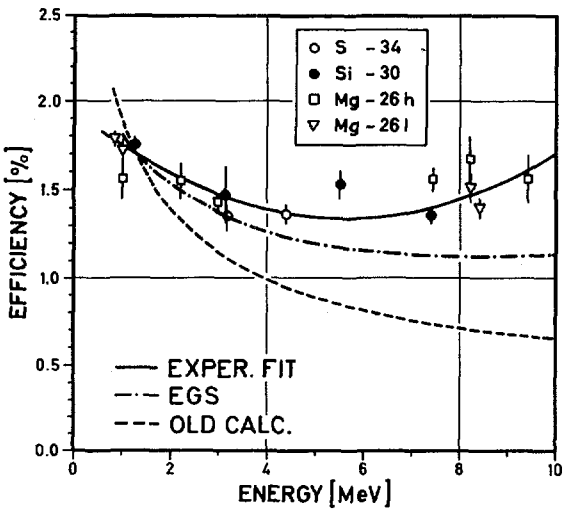

Fig.11. Absolute efficiency of the C_6D_6 scintillator plotted versus γ-ray energy for one experimental and two calculated data sets

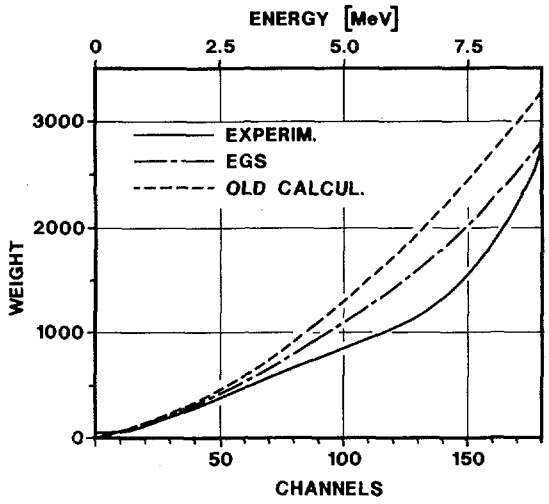

Fig.12. Weighting functions corresponding to 150 keV bias, normalized to same values at channel 10

The value of the 1.15 keV capture area computed with this W-function is $g\Gamma_n\Gamma_\gamma/\Gamma = (61.8 \pm 2.3)$ meV, i.e. about 11 % larger than the ORNL transmission value. One can therefore conclude that, for the Geel setup, the EGS calculations fail to reproduce the transmission values of the 1.15 keV resonance parameters.

One important aspect of the EGS calculations is to have pointed out the important rôle played by the surroundings and in particular by the sample acting as a source of high-energy electrons and positrons which can subsequently escape and be detected with high efficiency in the scintillator. In order to investigate this point, some measurements were carried out using as a source of almost monochromatic high-energy γ rays the resonance produced in the reaction $^{30}Si(p,\gamma)$ at E_p = 0.62 MeV. The compound state of ^{31}P corresponding to this resonance decays to the ground state with a 95 % branching ratio via a transition of energy E_γ = 7.898 MeV. The relative efficiency of this γ ray was measured versus the backing thickness in the geometry shown in the lower and right-hand side of Fig. 13, reproducing the neutron capture setup: up to three tantalum disks each 0.3 mm thick were added to the normal backing.

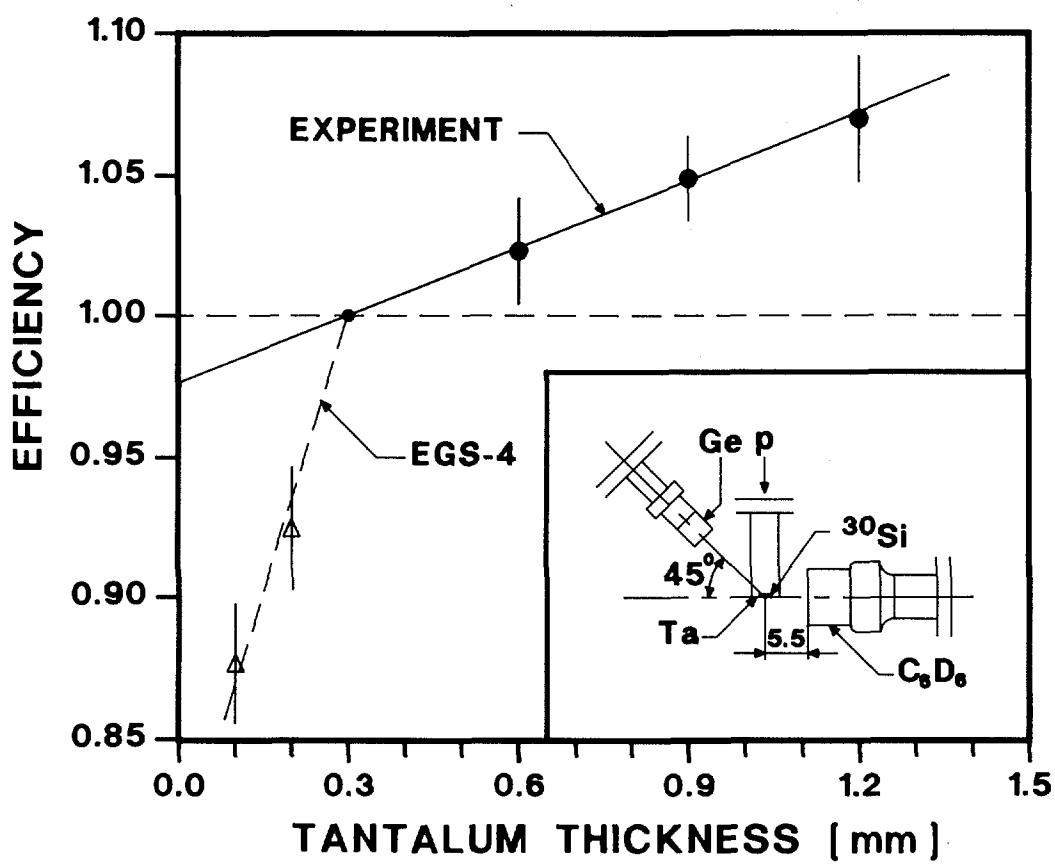

Fig.13. Comparison of measured and calculated values of the relative efficiency plotted versus the thickness of tantalum backing. Data are normalized to unity at a thickness of 0.3 mm.

Normalization to the same number of captures was achieved by measuring the full peak area of the 7.898 MeV transition in the γ-ray spectrum. The results, plotted in Fig. 13, show a very slight increase of the efficiency with thickness : for a total additional thickness of 0.9 mm tantalum, only a 7 % increment of the counting rate is observed. After weighting, even this small increase disappears. On the other hand some EGS calculations performed for thicknesses smaller or equal to 0.3 mm (see Fig. 13) point to a much higher slope of the efficiency versus thickness curve.
Also, a test was performed on the influence of the canning which, for the Geel detectors, consists of 2 mm thick aluminium walls and a teflon expansion tube filled with scintillator. The test consisted of replacing the C_6D_6 with an uncanned plastic scintillator and measuring the count rate of this detector with and without the canning, in the geometry of Fig. 13: an increase of 10 % due to the canning was observed.
Finally, a new (p,γ) measurement campaign has been carried out in order to determine the weighting function for the geometry of the neutron capture setup, in which two C_6D_6 detectors are placed symmetrically at 90° with respect to the beam and at 5.5 cm distance from the sample centre. The analysis is still in progress but preliminary results appear in good agreement with the previous ones obtained with one detector only, placed at an angle of 125° with respect to the proton beam.

NUCLEAR DATA FOR FUSION TECHNOLOGY

Double-Differential Neutron-Emission Cross-Sections

H. Liskien, L. Mewissen*, F. Poortmans*, J. Wartena, H. Weigmann

Double-differential neutron-emission cross section data for the 1 to 16 MeV incident neutron energy range are requested for neutron transport calculations in the blanket of a fusion reactor. Materials which will most likely be used in significant quantities in the blanket are lithium as the tritium breeding material through the reactions $^{6}Li(n,\alpha)t$ and $^{7}Li(n,n'\alpha)t$, beryllium or lead as neutron multipliers through the (n,2n) reactions, and the main structural materials iron and nickel.

The double-differential neutron emission cross sections are measured using the mercury-cooled uranium target of GELINA as a pulsed white neutron source. The accelerator is operated at a repetition rate of 800 Hz, an electron burst width of less than 1 ns, and an average beam power of 8 kW. The scattering sample is positioned at 60 m from the neutron source. The incident neutron beam is collimated to a diameter of 5 cm. Samples are mounted in a 2.5 m long thin-walled aluminium vacuum tube to reduce air-scattering of the incoming neutrons. The secondary neutrons are detected with eight NE 213 liquid scintillators surrounding the sample at a distance of 20 cm. Pulse shape discrimination is applied to separate neutrons from γ-ray events.

The incident neutron energy is determined by the time-of-flight method, in which the stop signal is derived from the detection of a secondary neutron. The energy spectrum of the secondary neutrons is determined by unfolding the pulse-height distributions observed in the NE 213 detectors. The shape of the incident neutron flux is measured with a ^{235}U fission chamber placed in the neutron beam at 30 m from the Linac target. Absolute cross sections will be obtained by normalization to the diferential-elastic scattering cross-section of ^{12}C below 2 MeV.

The experimental set up and the applied procedures have been described elsewhere(1). A series of measurements on the double-differential neutron emission cross-sections of ^{7}Li have been published(2), and a first run on ^{9}Be had been performed in 1986.

---

* SCK-CEN, Mol, Belgium

(1) E. Dekempeneer, H. Liskien, L. Mewissen, F. Poortmans, Nucl. Instr. Methods Phys. Res. A256 (1987) 489

(2) E. Dekempeneer, H. Liskien, L. Mewissen, F. Poortmans, Nucl. Sci. Eng. 97 (1987) 353

Since then the activity has been discontinued due to the engagement of the involved staff in other projects. It is hoped that the measurements on ^{9}Be can be taken up again in 1989.

(n,p) and (n,α) Excitation Functions for Molybdenum Isotopes

H. Liskien, S.M. Qaim*, R. Wölfle*

Molybdenum is an important component of structural materials for fission and future fusion reactors. Interaction of fast neutrons with molybdenum leads to the formation of many radioisotopes of molybdenum, niobium and zirconium. This work deals with such activation products with half lives between 0.7 and 70 days, and their formation cross sections for neutrons between 12 and 20 MeV are determined.

Neutrons were produced at the Geel Van de Graaff accelerator by the T(d,n) reaction, using the dependence of the neutron energy on the emission angle relative to the deuteron beam. Fifteen samples of metallic molybdenum, sandwiched between aluminium sheets, were placed at different angles. The neutron flux was determined by two methods : (1) a proton recoil telescope placed at an angle of 16° relative to the deuteron beam monitored the neutron flux, and the fluences at the sample positions were determined using the know neutron angular distribution of the T(d,n) source reaction; (2) the ^{24}Na activities induced in the aluminium sheets which sandwiched the molybdenum samples by the $^{27}Al(n,\alpha)$ reaction, were determined.

Table 3. Investigated activation products

Reaction	Nuclide	Half-life [d]	E [keV]	P
$^{92}Mo(n,\alpha)$	^{89}Zr	(3.268 ± 0.003)	909	(0.9904 ± 0.0003)
$^{92}Mo(n,p)$	^{92m}Nb	(10.15 ± 0.02)	935	(0.9915 ± 0.0004)
$^{92}Mo(n,np)$	^{91m}Nb	(62 ± 2)	1205	(0.034 ± 0.005)
$^{95}Mo(n,p)$	^{95g}Nb	(34.97 ± 0.03)	766	(0.9994 ± 0.0003)
$^{95}Mo(n,p)$	^{95m}Nb	(3.61 ± 0.03)	236	(0.250 ± 0.006)
$^{96}Mo(n,p)$	^{96}Nb	(0.973 ± 0.002)	1091	(0.494 ± 0.020)
$^{98}Mo(n,\alpha)$	^{95}Zr	(64.02 ± 0.04)	757	(0.546 ± 0.003)
$^{100}Mo(n,\alpha)$	^{97}Zr	(0.704 ± 0.002)		
	^{97}Nb		685	(0.9809 ± 0.0011)

* KFA, Jülich, Germany

The reaction products were identified at KFA Jülich, and their induced activities were determined using a calibrated 35 cm^3 Ge(Li) detector. The investigated reaction products are listed in Table 3 together with their decay characteristics (half-life, main γ ray measured, and branching ratio for this γ ray), and the main production reaction. Due to the use of samples with natural isotopic composition essentially all the activation products can be produced by some minor reaction path in addition to the main production reaction, and the resulting cross sections are thus correctly described as sums of the respective individual cross sections.

Experimental Excitation Function for ^{52}Cr(n,2n)

H. Liskien, M. Uhl*, M. Wagner*, G. Winkler*

The reaction ^{52}Cr(n,2n) leads to the well-known nuclide ^{51}Cr with a half-life of 27.7 days. Using the activation method and monoenergetic neutrons

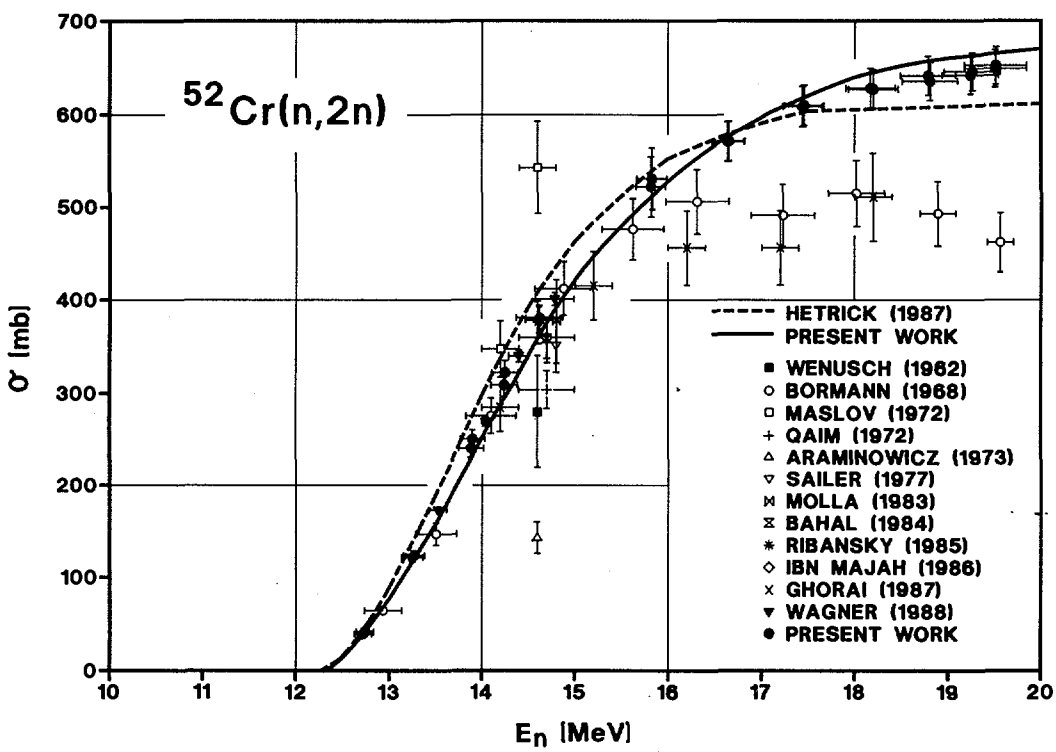

Fig. 14. Excitation function for the reaction ^{52}Cr(n,2n)

---

* IRK, Vienna, Austria

from the $T(d,n)^4He$ reaction the excitation function has been determined in cooperation with IRK Vienna. The neutron fluences at the 24 sample positions were determined relative to the n-p elastic scattering process employing a recoil proton telescope and relying on the well-known angular distribution for the neutrons from the T(d,n) reaction. Resulting cross sections are shown in Fig. 14; they are consistent with unpublished results from a cooperation between IRK Vienna and Kossuth University Debrecen at ~ 14 MeV and consistent with own recent theoretical calculations and earlier ones by Hetrick et al.[1]; they disagree above 15.2 MeV with the results recently published by S.K. Ghorai et al.[2]. A publication of the present work is in preparation.

Measurements of Double Differential (n,α) Cross-Sections

E. Wattecamps

Measurements of double differential (n,α) cross-section ratios of ^{60}Ni, ^{nat}Ni, ^{63}Cu and ^{65}Cu relative to ^{58}Ni, with neutrons of 14 MeV energy, were done with the multitelescope at the Van de Graaff accelerator. Similar measurements with neutron energies from 5 to 10 MeV were described earlier. The α-particle spectrum is measured in energy bins of about 0.5 MeV and for five angles. By integration over the emission angle and over the α-particle energy spectrum, the α-particle production rate ratio of the unknown sample relative to ^{58}Ni is deduced. These ratios are illustrated in Fig. 15, together with data deduced from measurements made by other laboratories. Our data have quite small error bars, and agree within error bars with the data deduced from the literature. Double differential data of α-particle yield versus α-particle energy and versus emission angle will be made available after completion of the energy loss correction of α-particles in the sample and in the telescope.

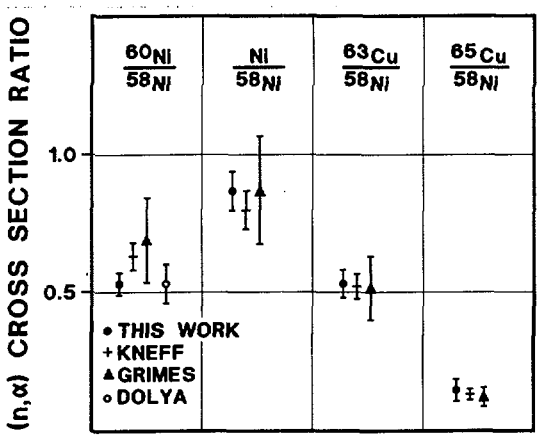

Fig. 15. Measured α-particle production cross-section ratio at 14 MeV

(1) D.M. Hetrick, C.Y. Fu, D.C. Larson, Oak Ridge National Laboratory Report ORNL/TM-10417 (1987)

(2) S.K. Ghorai, J.R. Williams, W.L. Alford, J. Phys. G : Nucl. Phys. 13 (1987) 405

Prior to the release of these data, together with similar double differential cross-section data already measured for neutron energies between5 and 10MeV, an additional measurement of Ni(n,α) at 8 MeV will be performed with a novel telescope to investigate why our α-yield data be performed with of ^{58}Ni at 8 MeV neutron energy are 20 % lower than any other measurement, whereas our measured data for copper agree well with literature values. The novel telescope has additional discrimination possibilities by time-of-flight and is described in the next section.

Development and Test of a ΔE-ΔE-E Alpha-Particle Telescope with Time-of-Flight Discrimination

E. Wattecamps, G. Rollin

The measurement of neutron induced charged particle cross-section data is needed for the design of first wall and other structures of fusion reactors.

It requires very specific and efficient detection systems if one is to determine the type of the particle, its energy and its emission angle. In the past (n,α) and (n,t) cross-section measurements were performed at the Van de Graaff accelerator with a multiangle telescope. A new telescope was designed which takes advantage of the recently installed 200 ps burst-width of the Van de Graaff accelerator. The aim is a better discrimination among different light ions, better background rejection, and higher efficiency.

The set up of the telescope in front of the D(d,n) target is shown in Fig. 16. A sample of 5 cm diameter (nickel or tantalum), or a ^{241}Am source are set at 8 cm distance from the deuterium gas cell.

A Multi Wire Parallel Plate Avalanche Counter MWPPAC1 of 5 cm diameter and 0.6 cm gap width, is located at 3 cm distance from the sample. A second, identical, MWPPAC2 is located at 23 cm from the first, in line with a Pilot U plastic scintillator of 3 cm diameter on a RCA 8850 PhotoMultiplier (PUPM). The scintillator of 0.1 cm thickness is at 25 cm distance from MWPPAC1.

The performance of the telescope can be characterised by the data obtained with mono-energetic α particles from the ^{241}Am source set at the sample location : (1) the pulse height resolution of the PUPM chain is 19 %, that of MWPPAC1 + MWPPAC2 is 54 %; (2) the time resolution of MWPPAC1, MWPPAC2 and PUPM is 640, 485 and 180 ps at FWHM, respectively.

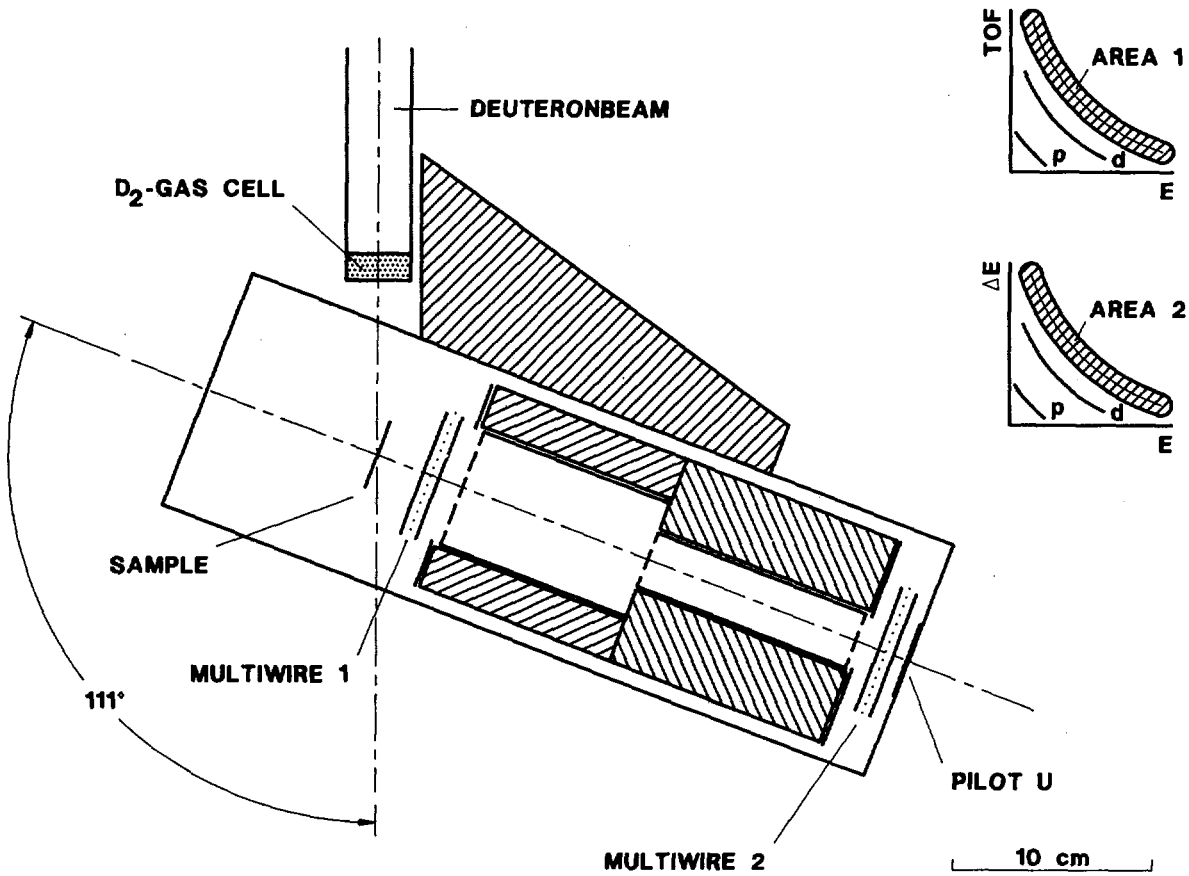

Fig. 16. Set up of the telescope in front of the D (d,n) target at the Van de Graaff accelerator

This last result still has to be confirmed. Therefore a special test bank was designed to investigate the time resolution limitations of current photomultipliers and plastic scintillators on various light guides.
The three detectors of the telescope are linked by a complex system of coincidences and gates to a multiparameter data acquisition system ND6600. This system acquires four parameters from any event in listing mode, namely :

- sum of energy loss in MWPPAC1 + MWPPAC2, ΔE,
- enrgy deduced from pulse height of PUPM, E,
- time of flight between target and MWPPAC1, TOF1, and
- time of flight between target and PUPM, TOF2.

The data acquisition system provides two-dimensional spectra of TOF2 versus E, and ΔE versus E. The particles of interest are confined to well defined areas, AREA1 and AREA2 (inserts of Fig. 16).

After two hours of irradiation of a nickel sample, and a subsequent irradiation of a tantalum sample for the same amount of fluence, the two data sets were sorted and analysed. Accepting only data within AREA1 and AREA2 (inserts of Fig. 16) and integration over time and energy loss, respectively, yields the foreground nickel and background tantalum energy spectra. The counting rate is reasonably high and the background is particularly small even at low energies.
An automated system of sample changer and data acquisition was designed but not yet tested. This will be essential for long runs with the already automated Van de Graaff accelerator.

Parametric Investigation of the Time Resolution of Plastic Scintillator Detectors

E. Wattecamps, G. Rollin

The energy resolution of time-of-flight measurements is proportional with the time resolution, inversely proportional with the flight-path length, whereas the counting rate decreases quadratically with the flight path length. To perform spectrum measurements within a reasonable measuring time with the required energy resolution, it is therefore preferred to have good timing accuracy of the start-stop devices instead of increasing the flight-path length. The burst width of the pulsed beam of the Van de Graaff accelerator is about 200 ps FWHM, and a reasonable timing accuracy of the time-of-flight detectors should compare with this neutron burst width. A time resolution of even 100 ps is achievable for very small detectors and a narrow pulse-height range. However, for an improved charged particle telescope we need a detector size of at least 25 cm^2 and a good time resolution over an α-particle energy range from 1 to 10 MeV.
A test bank was set up to perform parametric investigations such as : scintillator type and size, light guide geometries, photomultiplier, timing circuits, etc. Two RCA 8850 photomultipliers of 51 mm diameter view a 10^4 Bq ^{94}Nb source which yields prompt γ-ray cascades (0.702 and 0.871 MeV).
Three detector combinations were investigated so far (see Fig.17) :

- small plastic scintillators of 25 mm diameter and 14 mm thickness,
- small scintillators (as above) on conical (48 and 36 mm diameter) perspex light guides,
- larger plastic scintillators of 48 mm diameter and 14 mm thickness on the light guides mentioned above.

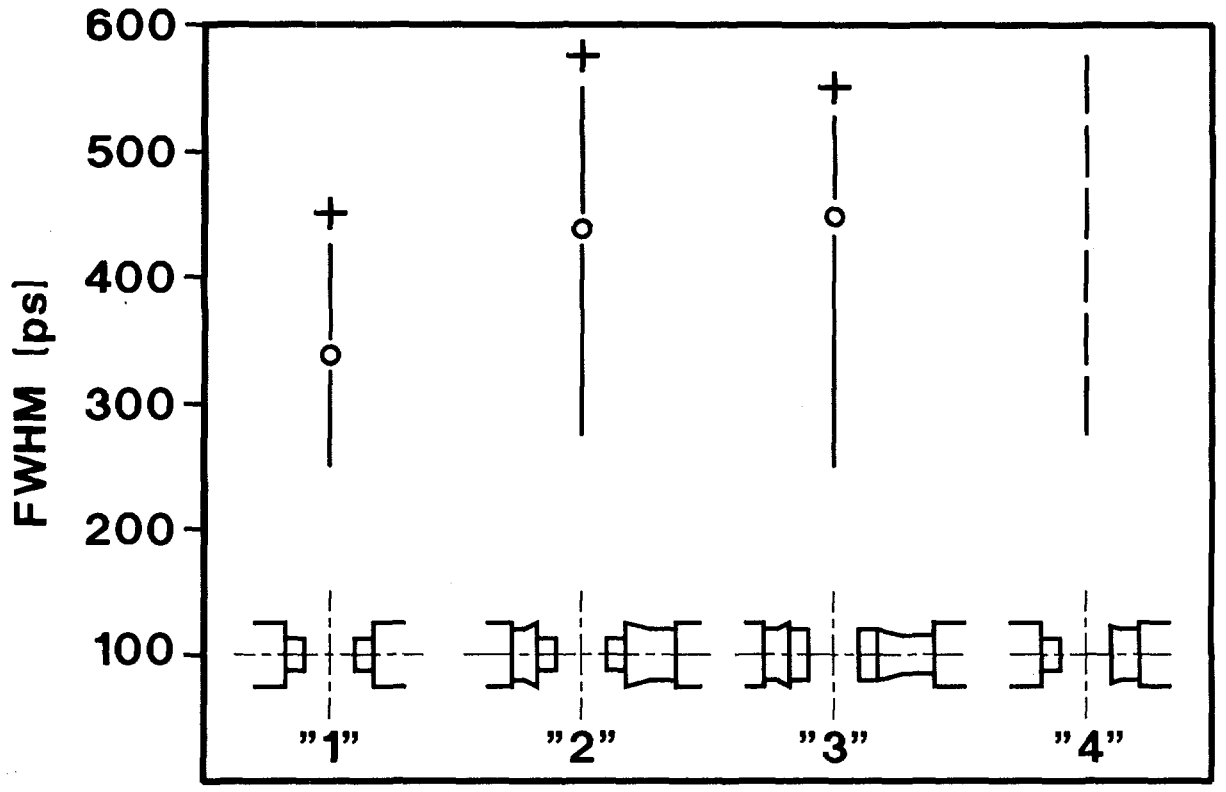

Fig.17. The FWHM of "Start-Stop" time distributions in ps. Geometry "1", "2" and "3" with ^{94}Nb. Geometry "4" with ^{241}Am is planned.
o pulse height windows : 1.4-1.6 and 1.4-1.6 volt
+ pulse height windows : 0.5-5.0 and 0.5-5.0 volt

The photomultipliers are mounted on conventional constant fraction timing discriminators ORTEC 270 with a conventional voltage divider. Optimum high voltage choice and careful settings of the CFD were repeatedly made. The electronics for both detectors is identical and consists of a slow, but linear and a separate fast chain. Start-stop time distributions versus pulse height were observed with a ND 6600 multiparameter acquisition system. A concise summary of the results is illustrated in Fig.17. A time resolution of 320 ps was obtained for a single detector chain, if the pulse height in both chains is within a pulse height window of 0.2 Volt at 1.5 Volt. Increasing the window on both chains increases the time resolution, caused in particular by the small pulses. Increasing the surface of illumination of the photocathode and increasing the size of the scintillator, increase the time resolution by about 80 ps and 40 ps respectively.

It is planned to investigate a fourth case, see also Fig.17, with a ^{241}Am source viewed by a gamma scintillator and by a thin Pilot U scintillator for the associated α particle.

SPECIAL STUDIES

Discontinuities of the Level Spacing in $^{50}Cr + n$ and $^{52}Cr + n$ Resonances

G. Rohr, R. Shelley, A. Brusegan, F. Corvi, F. Poortmans*, L. Mewissen*

Non-statistical effects for neutron resonances have been observed in the distribution of the level spacing as a function of neutron energy for both even isotopes. An abnormal increase of the level density as a function of the excitation energy for ^{50}Cr resonances is shown in Table 4, wherein N is the number of s-wave resonances and D_o their spacing for bins of 200 keV. The expected change in the level density with the energy is given by D_{th} calculated on the basis of the Bethe level density expression. The larger change of D in the (600-800) keV interval compared to that for the (0-200) keV range, can be interpreted by the level density systematics developed at CBNM Geel[1]. In Fig. 18 the energy distribution of the cumulative number of ^{52}Cr s-wave resonances, unexpectedly, is not linear. Two gaps are apparent, at (140-265) keV and (610-740) keV, where at least two resonances for each gap are lacking. The probability for two such gaps has been estimated to be 0.2 % by means of a Monte Carlo code based on a Wigner distribution.

Table 4. Excited levels in ^{50}Cr

Energy Range	N	D_o [keV]	D_{th} [keV]
0 - 200	11	18.2 ± 2.9	18.2
200 - 400	11	18.2 ± 2.9	16.1
400 - 600	16	12.5 ± 1.6	14.3
600 - 800	20	9.1 ± 1.0	12.7

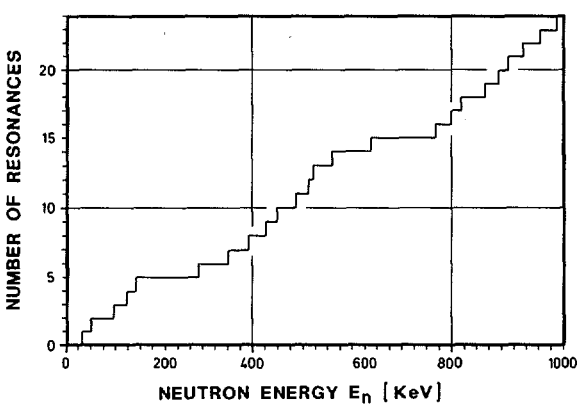

Fig. 18. Number of ^{52}Cr s-wave resonances as a function of neutron energy

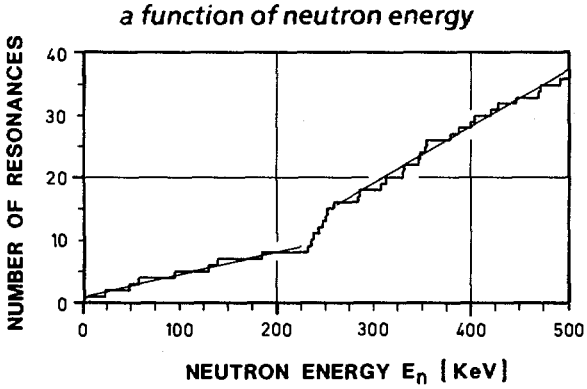

Fig. 19. Number of ^{52}Cr p-wave resonances as a function of neutron energy

---

* SCK/CEN, Mol, Belgium

(1) G. Rohr, Z. Phys. A318 (1984) 299

Another even stronger discontinuity of the level spacing is observed for p-wave resonances as shown in Fig. 19. If, in the range up to 500 keV only resonances definitely assigned as p-waves are considered, two regions can be distinguished where the cumulative level distribution is linear, namely the intervals (0-200) and (300-500) keV. The ranges are separated by a clustering of p-wave resonances at about 250 keV.
All these effects contradict the Bohr compound model, and the deviations from the statistical properties of the level spacings will allow the study of the two body interaction of nucleons in nuclei. The final results of ^{52}Cr+n have been published recently.

Nuclear Energy Level Spacing Distributions in Even Iron Isotopes

G. Rohr, R. Shelley, G. Vanpraet*

Nearest level spacing distributions of s-wave neutron resonances in ^{54,56}Fe and ^{58}Fe have been studied. It is found that for ^{54}Fe and ^{58}Fe the distribution of the observed individual level spacings deviates from a Wigner distribution. For ^{56}Fe such a deviation could not be verified in an unambiguous way. The reason for this may be that in ^{54}Fe and ^{58}Fe we are dealing with doorway resonances whereas in ^{56}Fe a mixing of 3p-2h energy levels belonging to neighbouring doorway state resonances is already effective.

New Aspects of Nuclear Level Spacing Distributions

G. Rohr

Neutron resonances of the 4n target nuclei ^{28}Si, ^{32}S, ^{40}Ca, ^{52}Cr and ^{96}Zr were studied. According to the independent particle model the excited states of these nuclei are created in one or two collisions and are the best candidates for studying the properties of nucleon-nucleon interaction in nuclei. It is shown that the doorway resonances and resonances originating from the same doorway state result in a Gaussian-like nearest level spacing distribution. The strong energy correlation between resonances is assigned to the nucleon-nucleon interaction and contradicts the independent particle picture. The almost equally spaced doorway states are important, since they fulfil in place of equidistant single particle states the rather simple assumption of the Bethe level density

---

* RUCA, Antwerpen, Belgium

formula. Furthermore, they explain the steps in the level density systematics, which is a pre-assumption for the prediction of level spacings for nuclei which are not measurable. An oral presentation has been given at the International Conference on Nuclear Data for Science and Technology in Mito, Japan, May/June 1988.

Gaussian-like Distribution of Neutron Resonance Levels

G. Rohr, R. Shelley, L. Mewissen*, F. Poortmans*

The light and closed shell nuclei have often been excluded when studying the average level spacing D and the level spacing distribution as the number of neutron resonances is small and therefore D is not well defined. However according to the independent particle model the excited states of these nuclei are created in one or two collisions and should be the best candidates in studying the properties of two body forces. It can be shown that almost all light nuclei, where a sufficient number of s-wave resonances is detected, have sequences of almost equally spaced resonances. According to this the level spacing inside the sequence is distributed like a Gaussian function, and a small number of resonances is sufficient to determine D. This property of particle excited states is due to the two body interaction and has been observed for ^{28}Si, ^{32}S, ^{40}Ca, ^{51}V, ^{52}Cr, ^{54}Fe, ^{56}Fe, ^{58}Fe and ^{96}Zr. This residual interaction seems to be also effective for medium- and heavy-mass nuclei where a large occurence of level spacings larger than the average level spacing with non-statistical character is observed.
Therefore, the presence of equally spaced resonances seems to be a universal property of nuclei. It proofs the independent particle model in neutron reactions and favours a regular motion of nucleons in the nucleus. The consequences of this unique property of particle excited states for nuclear physics have been discussed at the Frühjahrstagung des Fachausschusses Kernphysik der DPG in Berlin, Germany, March 1988.

* SCK/CEN, Mol, Belgium

NUCLEAR METROLOGY

RADIONUCLIDE METROLOGY

International Comparison of Activity-Concentration Measurements of a ^{125}I solution

D. Reher, T. Altzitzoglou, E. Celen, B. Denecke, D. Mouchel

On behalf of Section II (Mesures des Radionucléides) of the CCEMRI the BIPM launched an international full-scale comparison of activity-concentration measurements of a ^{125}I solution. It was the follow-up of the trial comparison which took place in 1987[1].

During the past years, the nuclide ^{125}I has been widely used in nuclear medicine. It decays by electron capture to an excited level of 35.5 keV in ^{125}Te, which de-excites by a highly converted isomeric transition. Although ^{125}I has a simple decay scheme, it is rather difficult to standardize because of the low energies of the radiations emitted and the frequently present ^{126}I impurity.

CBNM participated in this comparison using four measuring systems: (1) 4π-CsI(Tl) spectrometer, (2) 152 x 152 mm NaI(Tl)-well spectrometer, (3) a coincidence counter composed of two 51 x 51 mm NaI(Tl) detectors, and (4) an efficient (38 %) HP Ge spectrometer. With these instruments, four different methods were used to assess the activity of the ^{125}I sources; these are: (A) the sum-peak method, (B) the coincidence counting, (C) the photon-photon coincidence efficiency extrapolation technique, and (D) the total emission rate determination. The following combinations of methods and instruments were possible: 1A, 1D, 2A, 3A, 3B, 3C and 4A.

With the assumption that the efficiencies to detect gamma and X rays are equal, $\varepsilon_\gamma = \varepsilon_X$, for the three coincidence methods (A,B,C) the equation to determine the disintegration rate of a source has typically the same form: $M = N_0\ K\ f$, where M is the measured count rate, N_0 is the disintegration rate, f is a function of measured data, and K = 1.0193 + 0.0022 is a correction factor which contains only data from the decay scheme. This is a limiting factor for the accuracy of these methods.

With these techniques, we were able to provide results for the activity concentration of the ^{125}I solution, and, in addition, could compare the different methods with each other. A comparison of our results with those of the other participants is shown in Fig. 20.

---

(1) NEANDC (E) 292"U" Vol.III Euratom, INDC(EUR) 022/G (1988), p.38

A comparison of the various techniques with each other showed that integral counting of sufficiently thin sources (D) is the most accurate one, whereas the other three methods are significantly less accurate. Each of the three coincidence methods has, apart from the limiting factor K, some significant draw-backs. For the sum-peak method (A) the separation of the two peaks is not trivial, because under the "single-events" peak there are also sum peak events. Furthermore, the assumption, that the efficiency of the gamma and the X rays are equal, does not hold in all cases. The photon-photon coincidence-counting method (B), is rather sensitive to the assumption $\varepsilon_\gamma = \varepsilon_X$. For the photon-photon coincidence-efficiency extrapolation technique (C), there are problems concerning this assumption but also with the extrapolation of $\varepsilon \rightarrow 0$ over a long range. The data points in the vicinity of the extrapolation end-point have the highest uncertainty. Consequently, this method provides the least accurate results.

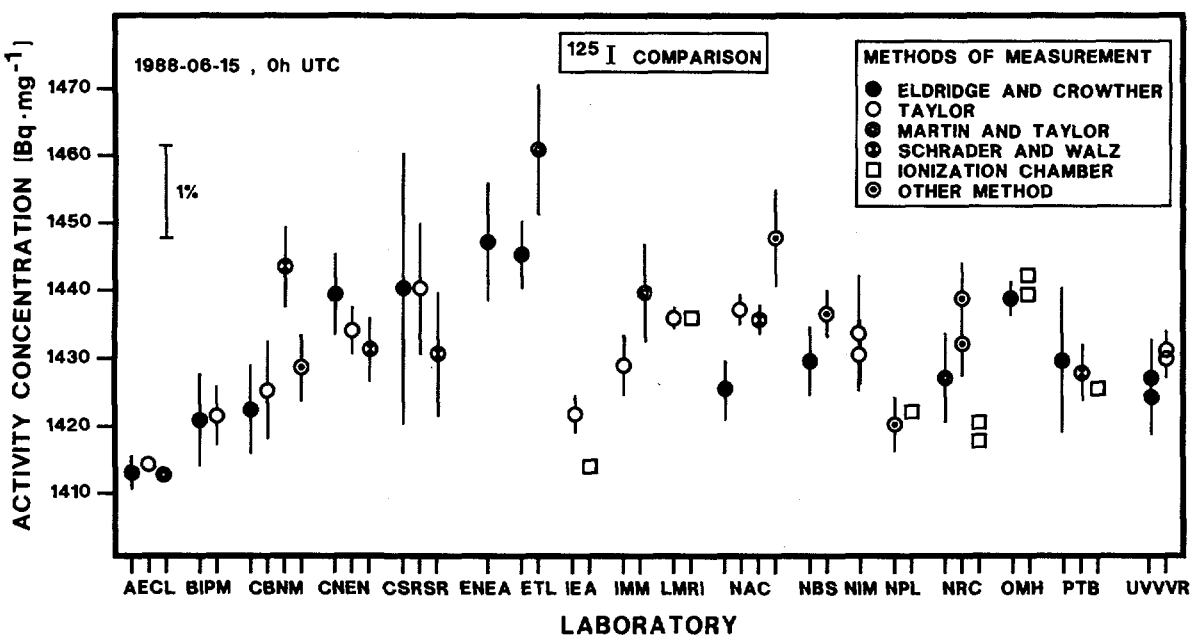

Fig.20. Results of the ^{125}I comparison (private communication, BIPM)

Analysis of Complex Alpha-Particle Spectra

E. Axton*, G. Bortels

An interactive version of the CBNM code for analysing alpha spectra has been written in APL for use on the CBNM mainframe. The fitting model is unchanged[1] but the least-squares solution is obtained via a Cholesky factorization and Hausholder transformation[2] which provide improved numerical stability. This means that small peaks in a multiplet can more easily be analyzed simultaneously with the large peaks. In addition, more flexibility is obtained since a larger number of parameters can be optimized simultaneously. The code calculates peak areas and energies, the latter after a pulser calibration for each spectrum. In this way, corrections can be made for monotonic drift over long measurement cycles. Mean values and uncertainties from a covariance analysis are calculated for sets of spectra analyzed successively.

Low-Energy X-Ray Standards

B. Denecke, G. Grosse, C. Ballaux**

With the improvements of the low-geometry X-ray counting system, announced in the previous progress report[3], and with additional refinements, it was possible to calibrate five Al-fluorescence sources for their X-ray emission rate (range: 10^3 to 10^5 s^{-1}). At the moment, the total uncertainty is estimated to be 3 %.

In addition, the following achievements and observations were made : for long counting periods (several hours), the gain shift from gas-density variations is reduced to about 0.5 %. This has been achieved by temperature stabilization of the thermally insulated counter and pressure-reference vessel by forced water circulation with a bath thermostat.

Depending on the Ar-CH_4 gas-flow rate, the gas gain can decrease up to 20 % due to the permeation of hydrogen from the source chamber through the counter window. With helium gas, this effect is not observed. Therefore, helium will be used in future in the source chamber and an Ar-CH_4 mixture in the counter for the measurements of KX-rays with an energy above 3 keV.

---

* Scientific Visitor from NPL, Teddington, United Kingdom, retired

** SCK/CEN, Mol, Belgium

(1) G. Bortels, P. Collaers, Appl. Radiat. Isot. A 38 (1987) 831

(2) C. Bastian, in V. Piksaikin (ed.), Covariance Methods and Practices in the Field of Nuclear Data, INDC(NDS)-192/L, (1988), p.89

(3) NEANDC (E) 292 "U" Vol. III Euratom, INDC (EUR) 022/G (1988), p. 41

With CH_4 as counting gas, the gas gain is independent of the CH_4-flow rate when hydrogen or helium is flowing through the source chamber.
In order to verify the accuracy of the computed[1,2] detection efficiency, a series of measurements has been started in which the parameters used in the calculations are varied. These are: the type and composition of the various counter and source-chamber gases, the thickness of the polyimide counter window and the gas pressure.
The present type of sources suffer from the large contribution of the excitation Mn-KX rays, the intensity of which is much higher than that of the fluorescent Al-KX rays. In addition, the Mn-KX rays produce in the spectrum a considerable low-energy tail on which the fluorescent Al-KX rays are superimposed. This causes an additional uncertainty in the spectrum analysis which becomes difficult not only in the standardization of the reference sources but also in the efficiency calibration of Si(Li) detectors, at the aimed accuracy level of 5 %.

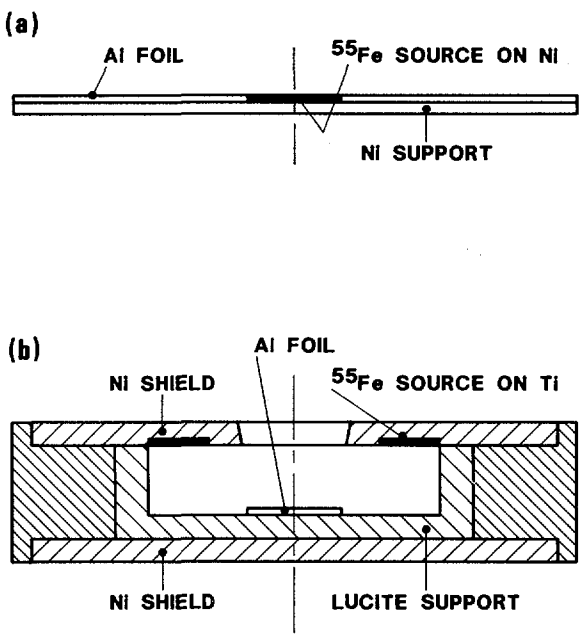

Fig.21. Low-energy KX-ray fluorescence sources. (a) 2π-geometry source, ^{55}Fe in direct contact with the fluorescer foil, (b) indirect source, ^{55}Fe shielded from the detector

To avoid the disadvantages of these sources, an improved type of fluorescence sources has been constructed (Fig. 21). The ^{55}Fe excitation source is deposited onto an annular titanium foil which enhances the excitation. This source is placed inside the top cover of a cylindrical nickel container. At the bottom center of the container, the fluorescer foil is placed on a lucite support. The fluorescent X rays can emerge from the source through a small aperture on top, allowing a solid angle of 0.3 sr to be subtended by the detector. With this type of sources, the detector is completely shielded against the Mn-KX rays. The envisaged fluorescence materials are manganese, aluminium, silicon, chlorine, calcium, scandium, titanium and vanadium. Prototypes of

(1) M. J. Berger, J. H. Hubbel, Report NBSIR 87-3597 (1987)
(2) W. Bambynek, Internal Report GE/R/RN/03/86 (1986)

these indirect sources have been successfully measured. The accuracy for the X-ray emission rate is expected to be better than 3 %.
The small corrections for impurity X-ray lines, which cannot be resolved by the gas-flow proportional counter, were determined from a measurement with an efficiency-calibrated Si(Li) detector.

Determination of the ^{238}U Mass of a 2 Bq Sample

B. Denecke

In a joint experiment of CBNM and the Institut für Radiumforschung und Kernphysik (IRK) of the University of Vienna, the neutron cross section of the $^{93}Nb(n,n')^{93m}Nb$ reaction was measured at a neutron energy of 8 MeV[1] using as reference the $^{238}U(n,f)/^{27}Al(n,\alpha)$ cross-section ratio. At IRK the mass of the used ^{238}U layer was determined by neutron irradiation using the $^{238}U(n,f)/^{27}Al(n,\alpha)$ cross-section ratio at 14 MeV. The result obtained was (167.6 ± 2.5) µg.
Alpha-particle counting in 2π geometry yielded a total emission rate of (2.01 ± 0.06) Bq. Using $(4.468 \pm 0.005)\cdot 10^9$ years as the ^{238}U half life[2] and estimating the ^{234}U impurity to be 2 %, the mass of the ^{238}U layer was found to be 158.4 µg.
It was decided to remeasure the ^{238}U mass of the sample at CBNM by alpha-particle spectometry at a defined low solid angle of (0.5146 ± 0.0005) sr.
An ion-implanted Si detector of 61 mm diameter with a resolution of 46 keV at 5.485 MeV was used as alpha-particle detector. The good resolution allowed to determine, in addition to the total count rate, the radionuclide composition of the sample from the spectral distribution of the detected pulses.
The source and the background were measured alternately for periods of several days. About $2.1\cdot 10^5$ counts were collected from the source and 175 counts as the detector background.
Using $(1.2436 \pm 0.0014)\cdot 10^4$ Bq/g as the specific activity of ^{238}U, and the measured ^{238}U activity, a mass of (159.7 ± 0.5) µg was deduced.

---

(1) NEANDC (E) 292"U" Vol.III Euratom, INDC(EUR) 022/G (1988), p.25
(2) E. Browne and R.B. Firestone, Table of Radioactive Isotopes, (John Wiley & Sons, New York, 1986)

This result is about 5 % lower than the value obtained from the neutron-irradiation method, and the uncertainties of both results do not overlap. The CBNM result agrees within 0.8 % with the alpha-particle counting method in 2π geometry. However, the latter method is less accurate due to the unsufficiently known corrections for scattering and self absorption. The value obtained at CBNM during a collecting time of about two months has a final uncertainty of 0.3 %, assuming that the half life of ^{238}U is correct within its stated uncertainty.

METROLOGY FOR NEUTRON FLUX AND DOSE

International Fluence Comparison

H.Liskien, Li Linpei*, R.Widera

In 1986 the Van de Graaff laboratory of CBNM participated in a BIPM fast neutron fluence intercomparison which used two uranium-loaded parallel-multiplate fission ionisation chambers as transfer instruments[1]. Triggered by the positive experience with these transfer instruments meanwhile an own pair of chambers has been built.

Each chamber (180 mm diam. x 80 mm) is made of 0.2 mm Inox and contains as electrodes thirteen tantalum sheets (90 mm diam. , 0.2 mm thickness) with 5 mm separation distance between neighbouring electrodes. They are operated at 120 V in continuous gas flow (90 % A, 10 % CH_4). In each chamber six electrodes are covered on both sides by U_3O_8 layers (76 mm diam., 0.4 to 0.6 mg/cm^2 thickness). The layers were made by suspension spraying. The ^{238}U-chamber contains material enriched to >99.98 atom% in ^{238}U, the ^{235}U-chamber material enriched to >97.6 atom% in ^{235}U. Unfortunately this latter material contains also 1.66 atom% ^{234}U which hinders a perfect separation of fission fragment from piled-up α particles. Tests have been performed in view of the timing properties for time-of-flight applications. Time resolution of about 10 to 12 ns were obtained.

Fields of quasi-monoenergetic neutrons are unavoidably accompanied by neutrons of degraded energy. Depending on the intensity of these neutrons and the energy behaviour of the neutron cross section curves involved, these unwanted neutrons necessitate very important corrections.

If the sources can not be pulsed, then there remain two other possibilities: (1) the multisphere method in which a slow neutron detector is placed in the centre of several moderating spheres of different diameters and therefore different response functions or (2) by mapping the neutron field and learning from the deviations from the $1/r^2$ law. Section III (Neutron Measurements) of CCEMRI/BIPM recommended to combine both above-mentioned methods and to test their usefulness in a mini-intercomparison. The provided detection system consisted of a spherical ^{3}He proportional counter of type SP90 and two surrounding moderating spheres of R_0 = 4.445 cm radius (small sphere) and R_0 = 12.065 cm radius (big sphere). Measurements were demanded for two of the standardized neutron energies, 2.5 and 14.8 MeV, and for distances (source - center of sphere) up to at least D_0 = 250 cm.

---

* Scientific Visitor from the National Institute of Metrology, Beijing, PR of China

(1) H. Liskien, A. Paulsen, R. Widera, S. Bao, CBNM Internal Report GE/R/VG/51/86

Using the $T(p,n)^3He$ reaction 2.50 MeV neutrons were produced by bombarding T-Ti layers with a proton beam from CBNM's 7 MV CN-type Van de Graaff accelerator and by positioning the moderating spheres in the 0° direction. Depending on the diameter of the moderator and the 'source - sphere' distance two different target thicknesses were used, 185 $\mu g/cm^2$ and 950 $\mu g/cm^2$. For both targets the accelerator voltage was adjusted such that the average energy of the protons in the T-Ti layer was 3280 keV. Ion currents up to 4 µA were used and integrated by a BIC model 1000 C unit. Only the 185 $\mu g/cm^2$ target was used to produce 14.80 MeV neutrons via the $T(d,n)^4He$ reaction. The average deuteron energy in the T-Ti layer was 750 keV taking into account the 25 keV energy loss in half the layer. The moderating spheres were positioned in the 74.4° direction relative to the deuteron direction. Ion currents up to 20 µA were used in this case.
The neutron source strength was monitored with a directional long counter from CEA Cadarache positioned at about 6.5 m and at an angle of 45° relative to the ion beam direction. Its background counting rate was determined to be 0.060 s^{-1}. It turned out that for a given day the source strength was proportional to the ion current within the statistical uncertainty of the monitor counts. Therefore, results from the same day were linked by the charge monitor, while results from different days were linked via the long counter. The absolute neutron fluence in the sphere direction (0° and 74.4°) has been determined for both neutron energies using CBNM's proton recoil telescope counter TC2.
The moderating sphere rests on three aluminium pins, its position is adjustable in all three dimensions by a cross slide system. The whole support is running on a rail system which allows source-sphere distances up to 500 cm. The angle between the rail direction and the ion beam direction has been adjusted using a goniometer. For distance determinations we used a VEB Suhl inside micrometer or a NEDO telescope meter. A typical obtained pulse height spectrum is given in Fig. 22. The lower counting threshold was set to 20 % of the peak pulse height, in accordance with the protocol. Counting rates never exceeded 3000 s^{-1} to keep the dead-time correction reasonably small.
Following the measurement protocol it had to be assumed that there are two background fields besides the main field. Firstly, a field of constant intensity and secondly, a field whose intensity varies with 1/r. Distances were introduced as dimensionless variable $x = D_O/R_O$.

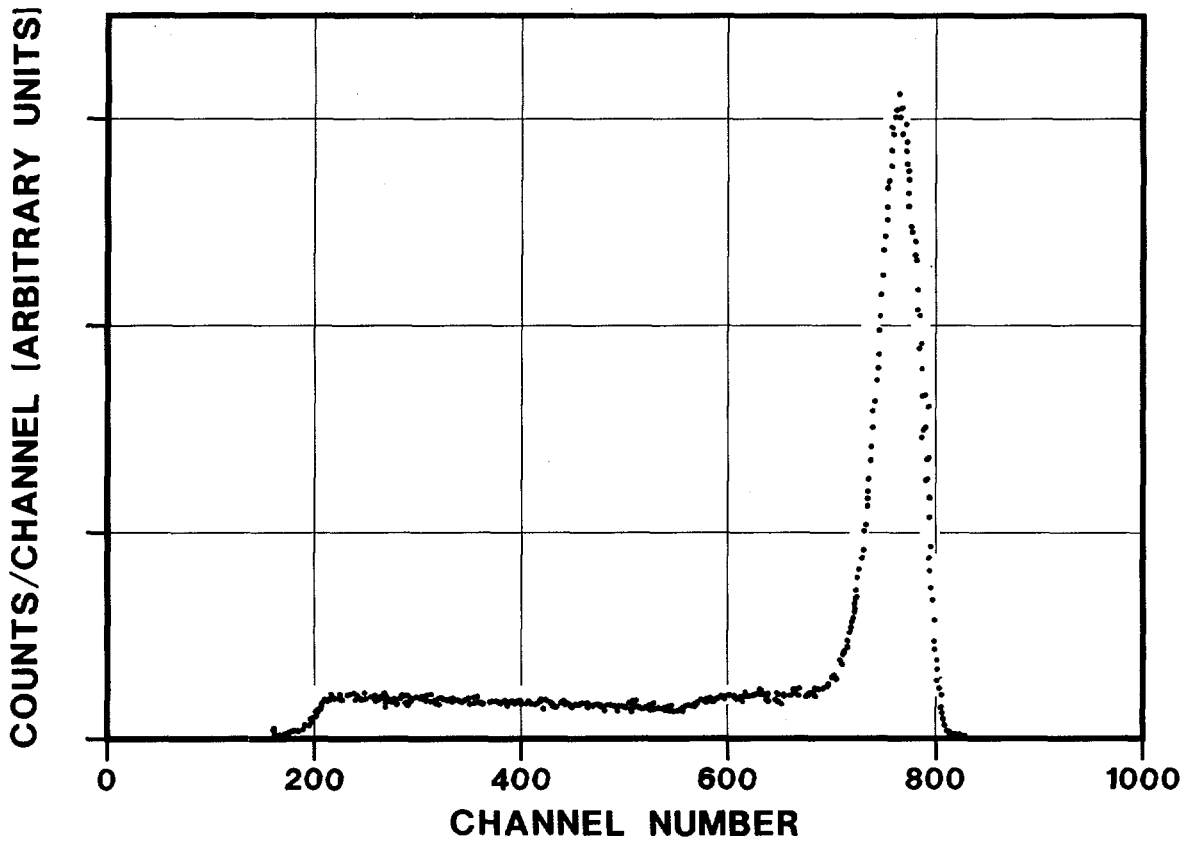

Fig.22. Typical pulse height spectrum obtained with the ^3He proportional counter

Corrected sphere counts per monitor counts (c) were multiplied with x^2 to obtain input data $y=c \cdot x^2$. This has the advantage of obtaining only slowly varying input data and allows to include - to a very good approximation - the distance uncertainty. Finally, the following ansatz was made :

$$y = p_1 \cdot [\ f_1(x) \cdot \{1 + p_2 \cdot f_2(x)\} + p_3 \cdot x + p^4 \cdot x^2\ ].$$

Direct neutrons are corrected for air attenuation following :

$$f_1(x) = 1 - \mu \cdot R_0 \cdot x.$$

Changes of the energy and intensity distribution of the neutrons from the main field as function of the changing solid angle between source and moderating sphere are thought to be described by the parameter p_2 and the function $f_2(x)$

$$f_2(x) = 2 \cdot x^2 \cdot [\ 1 - \{\ 1 - 1/x^2\ \}] - 1.$$

Fits have been performed with an existing BASIC programme (without taking into account the correlations) and a newly written APL programme (which takes into account the existing correlations). Results cannot be given in this report as the comparison is blind and other participating laboratories have not finished their work.

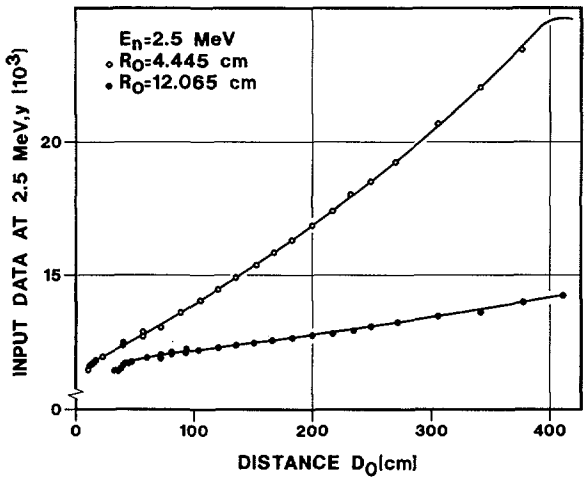

Fig.23. Input data and fit at 2.5 MeV for two different spheres

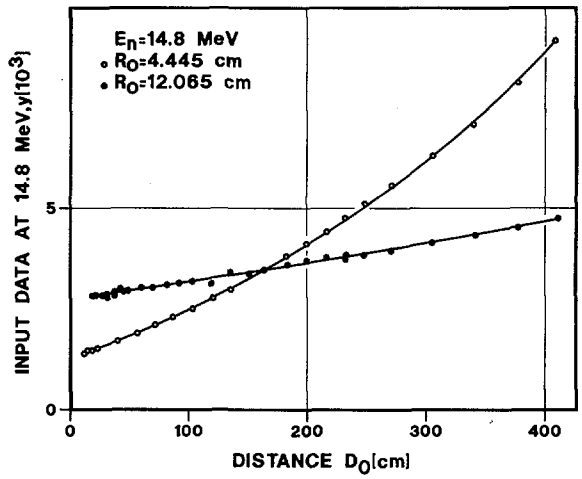

Fig.24. Input data and fit at 14.8 MeV for two different spheres

Input data at 2.5 MeV (see Fig. 23) can be described by the ansatz made. At 14.8 MeV the input data vary by a factor 6 (see Fig. 24) and the ansatz fails. Clearly, there is no really constant field (which should then exist also at very large distances!) and the assumption of a 1/r field is also debatable.

The efficiency ε of the detector plus the moderating sphere at any arbitrary distance D_0 can be defined as the ratio of counts per monitor counts (p_1/x^2) divided by the product of neutron fluence per monitor counts ($\varnothing/D_0^2$) and the sphere cross section ($R_0^2\pi$).

The efficiency at 2.5 MeV is independent of the sphere radius. This is not the case at 14.8 MeV. Obviously the diameter of at least the small sphere is insuffient for neutron moderation at this energy.

Neutron Dosimetry

H. Liskien, Li Linpei*, A. Paulsen**, R. Widera

Former cooperative work with SCK/CEN and the Catholic University of Louvain on the "Chromosome Aberrations Induced in Vitro in Human Lymphocytes by Monoenergetic 2.5 MeV Neutrons and ^{60}Co Gamma Rays" has been finalized and a short manuscript prepared. The found dose-response curve is given in Fig. 25.

Since then the modus of cooperation has been changed and we provide fast neutron fields and dose determinations on a pay basis. About thousand mice

---

* Scientific Visitor from the National Institute of Metrology, Beijing, PR of China

** Retired

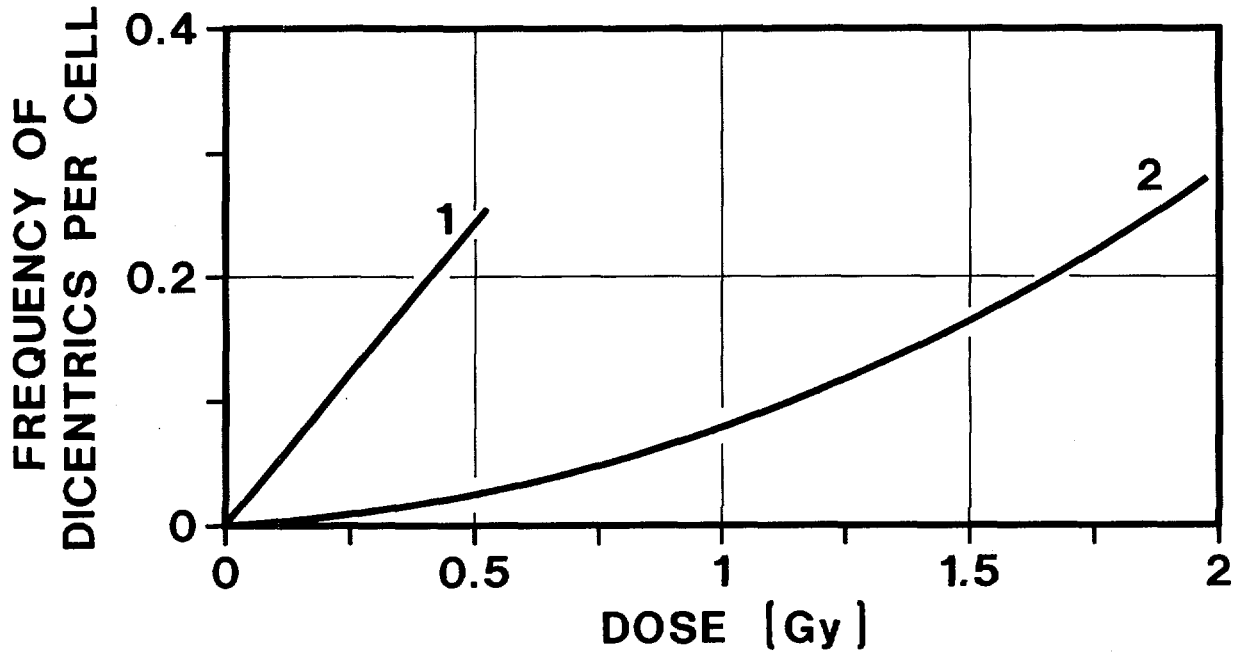

Fig.25. Dose-response curve of dicentrics per cell induced in human lymphocytes by monoenergetic 2.5 MeV neutrons (1) and ^{60}Co gamma rays (2)

have been irradiated with neutron doses of about 12.5, 25 and 50 cGy. These irradiations were performed at the new thick-target Be(d,n) field of the Van de Graaff at E_d = 6.3 MeV using a distance of ≈ 55 cm from the source and a pyramidal collimator (2.2 x 2.2 cm at the source and 14.1 x 14.1 cm at the sample position). The neutron spectrum extends to a maximum of 10.7 MeV, the average neutron energy being ≈ 3.1 MeV. The average dose has been determined for each irradiation with a 0.53 cm^3 thimble ionisation chamber operated in continous TE-gas flow by total charge determination using $\langle W \rangle$ = (31.9±1.5) eV. Small temperature and pressure corrections were applied. The accuracy was ± 7 %.

TECHNICAL APPENDIX

Electron Linear Accelerator

J. M. Salomé

The new high energy neutron target consisting of a pile of uranium and beryllium plates mounted in a beryllium cylinder is now ready and, according to the programme, will be tested on the accelerator beginning next year. At the origin, it was provided to cover the target with tantalum. Due to tightness problems and for safety reasons, the present target is surrounded by stainless steel and, as the other ones, mercury cooled.

Study of Transition Radiation

X. Artru*, P. Goedtkindt**, F. Poortmans***, J.M. Salomé, F. Van Reeth, C. Waller, L. Wartski*, N. Maene***

Transition Radiation (TR) is generated when energetic electrons cross the boundary between two media. The radiation can extend from microwave to X-

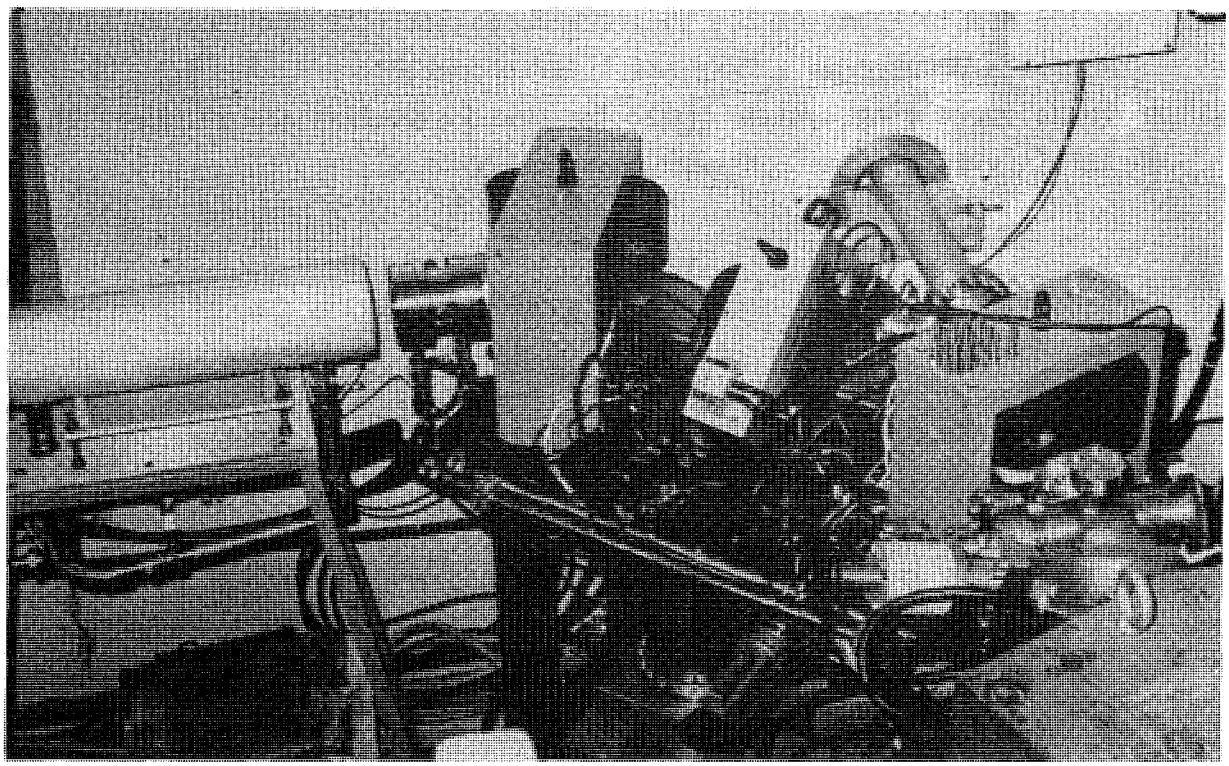

Fig. 26. The TR radiator followed by the X ray beam pipe and the 40 MeV electron beam deflector

---

* Université de Paris XI, Orsay, France
** EC Fellow
*** SCK/CEN, Mol, Belgium

ray frequencies. TR experiments were started this year by some irradiations of thin foils in the γ-ray-neutron field, close to the GELINA target and in the high power electron beam. Aluminium and havar foils are not damaged after 70 hours in a 65 μA - 100 MeV electron beam.
A transport system which magnetically deflects a 40 MeV electron beam was installed in place of the Photon Activation Facility (Fig. 26).
After passing through the foils, the electron beam is directed to a beam catcher while the forward directed X-ray beam can be detected in an outside room. Up to now, it was not possible to measure the X-rays due to the high bremsstrahlung background radiation.

Optical transition radiation is easily visible in a side direction when a foil is obliquely positioned to the particle beam. Such an experiment was realized and the typical "doughnut" observed.
Several experiments are being prepared :

(1) X-ray measurements at 40 MeV electron energy with one foil and a stack of foils (deflected beam),
(2) optical TR observation :
   - at 40 MeV, normally to the deflected beam,
   - at 100 MeV in front of the compression magnet with one foil or with two foils mounted as a "Wartski interferometer",
(3) an image processing system should be used to analyse the pictures in detail in view of electron beam characterization.

Van De Graaff Accelerators

A. Crametz

Preliminary dose measurements have been done on the R2 extension, to determine the shielding of a thick beryllium target for the permissible maximum ion beam intensity. For TOF experiments with a pulse repetition frequency of 0.625 MHz, the maximum current obtainable is 1.5 μA. This requires a shielding of 4 cm of copper plus 16 cm of paraffin in order not to overpass the thresholds fixed by the Health Physics group for the neutron and γ-ray detectors placed in the target hall. An internal report is in preparation.
KN-3.7 MV : Once the ion source has been exchanged. In the target hall, extensions r1 and r2 have been fully equipped for surface analysis experiments using ions as probe.

Operation of Central Computer System

C. Cervini, H. Horstmann

The central computer (IBM 4381/P2) is part of an integrated system for scientific data processing and office automation based on a standard IEEE 802.3 Ethernet, 3.6 km long (Fig. 27). The central computer is mainly used for batch processing and interactive work in order to analyse experimental data: Nuclear Measurements (91.8 %), Reference Materials (3.1 %) and Administrative Work (5.1 %).

Several APL2 programs have been developed in order to support the use of colour graphics on 3179G video displays, 6180 plotters and 3268/C2 printers.

The installation of modern hardware and software for telecommunication via packet-switched public lines has been prepared. Special software has been selected in order to connect the central computer to international networks, such as EARN, Bitnet, etc. For this connection OSI (Open System Interconnection) standards will be followed as far as possible.

Support for Office Automation

U. Meloni, J. Soro, P. Van Roy, H. Horstmann

The XEROX 8000 office automation system (Fig. 27) has been extended according to the needs for support of administrative and scientific work. For the time being the system is based on 25 workstations and 7 servers for filing, high-quality laser printing (3 x 2700) and communication. The workstations of the XEROX system can now be used for 3270 terminal emulation of the IBM 4381 mainframe.

The establishments of Geel, Karlsruhe and Ispra and the General Direction of the JRC at Brussels have been connected via packet-switched (X.25) public lines for electronic mail and document processing, in particular to support the service of financial control for the JRC.

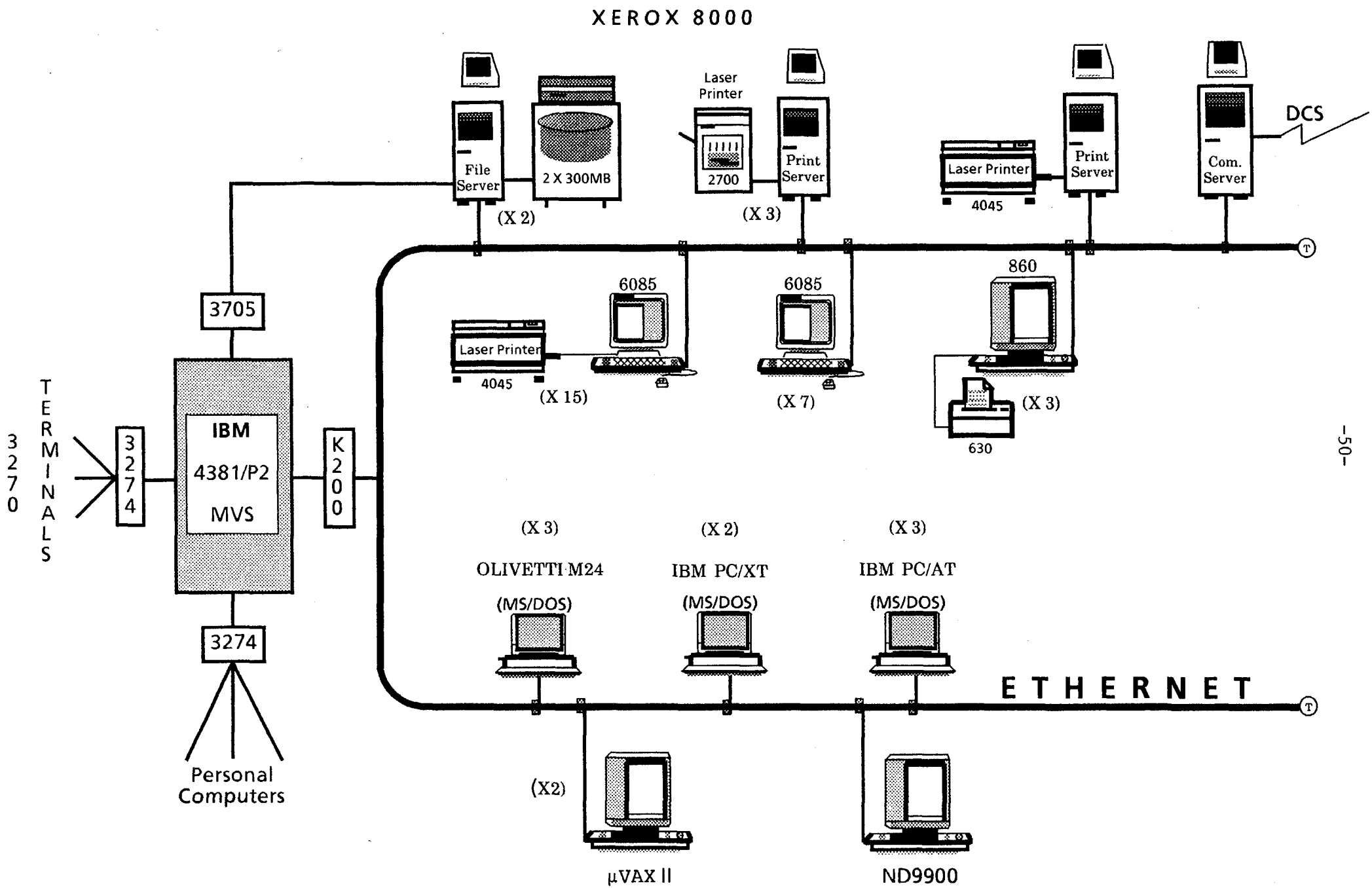
XEROX 8000
File Server
2 X 300MB
(X 2)
Laser Printer
2700
Print Server
(X 3)
Laser Printer
4045
Print Server
Com. Server
DCS
3705
6085
Laser Printer
4045
(X 15)
6085
(X 7)
860
630
(X 3)
3270 TERMINALS
3274
IBM
4381/P2
MVS
K200
3274
Personal Computers
(X 3)
OLIVETTI M24
(MS/DOS)
(X 2)
IBM PC/XT
(MS/DOS)
(X 3)
IBM PC/AT
(MS/DOS)
ETHERNET
(X2)
µVAX II
ND9900

LIST OF PUBLICATIONS

CONTRIBUTION TO CONFERENCES

BABELIOWSKY, T.
High-speed data transfer on Ethernet.
DECUS - SIG Treffen, München, September 26 - 30, 1988

BAMBYNEK, W.
Uncertainty assignment in radionuclide metrology.
Low-Level Measurements and their Applications to Environmental Radioactivity, Proc. 1st Summer School, La Rábida; M. Garcia-Leon and G. Madurga (eds.), World Scientific, Singapore (1988), p. 3

BAMBYNEK, W.
Radionuclide data.
Ibidem, p. 37

BÖCKHOFF, K.H.
The Geel electron linac and its potential in the framework of applications of nuclear technologies.
Intern. Conf. on Appl. of Nucl. Techniques, Crete, June 26 - July 2, 1988

BUTDZ-JØRGENSEN, C., KNITTER, H.-H.
Simultaneous investigation of fission fragments and neutrons in ^{252}Cf (SF).
IAEA Consultants Meeting on Physics of Neutron Emission in Fission, Mito, May 24-27, 1988

CORVI, F., FIONI, G.
Shape of the ^{238}U neutron captive cross section in the range 0.002-0.1 eV.
Nuclear Data for Science and Technology, Proc. Intern. Conf., Mito; S. Igarasi (ed.), JAERI, Tokyo (1988), p. 127

CORVI, F., PREVIGNANO, A., SMITH, B.P., GASPERINI, F.
Experimental determination of the response function of a gamma-ray detector in the range 0.5-10 MeV.
Capture Gamma-Ray Spectroscopy, Proc. 6th Intern. Symp., Leuven; K. Abrahams and P. Van Assche (eds.), Institute of Physics, Bristol and Philadelphia, Conference Series N° 88 (1988), p. 767

HAMBSCH, F.-J., KNITTER, H.-H., BUDTZ-JØRGENSEN, C., MUTTERER, M., THEOBALD, J.P.
Early and late stages of low energy nuclear fission fragment mass-, energy- and shape-fluctuations.
Collective Phenomena in Nuclear and Subnuclear Long-Range Interactions in Nuclei, Proc. Intern. Conf., Bad Honnef; P. David (ed.), World Scientific, Singapore (1988), p. 68

HAMBSCH, F.-J., KNITTER, H.-H., BUDTZ-JØRGENSEN, C., THEOBALD, J.P.
Interpretation of fluctuations of $\bar{\nu}$ and $\bar{E}_\gamma$ in resonances of ^{235}U (n,f).
IAEA Consultants Meeting on Physics of Neutron Emission in Fission, Mito, May 24 - 27, 1988

HAMBSCH, F.-J., KNITTER, H.-H., BUDTZ-JØRGENSEN, C., THEOBALD, J.P.
Fission fragment distributions in resolved resonances ^{235}U (n,f).
Nuclear Data for Science and Technology, Proc. Intern. Conf., Mito; S. Igarasi (ed.), JAERI, Tokyo (1988), p. 407

INGELBRECHT, C., PEETERMANS, F., PAUWELS, J., VAN AUDENHOVE, J.
A study of the homogeneity of aluminium - cobalt alloys for neutron dosimetry.
14th World Conf. of the Intern. Nucl. Target Development Society, Darmstadt, September 5 - 9, 1988

KNITTER, H.-H., BUDTZ-JØRGENSEN, C.
Experimental techniques for fission data measurements.
Nuclear Data for Science and Technology, Proc. Intern. Conf., Mito; S. Igarasi (ed.), JAERI, Tokyo (1988),p. 337

KNITTER, H.-H., HAMBSCH, F.-J., BUDTZ-JØRGENSEN, C., STRAEDE, C., THEOBALD, J.P.
Fission modes in ^{235}U (n,f).
Neutron Physics, Proc. Intern. Conf., Kiev; B.D. Kuzminov (ed.), ICSTI, Moscow, Vol. 3 (1988), p. 22

MAST, H., EYKENS, R., PAUWELS, J., WAGEMANS, C.
^{243}Am targets for nuclear fission experiments : requirements and realisation.
14th World Conf. of the Intern. Nucl. Target Development Society, Darmstadt, September 5 - 9,1988

ROHR, G.
Intruder states : result of different energy behaviour of intrinsic and collective states.
Capture Gamma-Ray Spectroscopy, Proc. 6th Intern. Symp., Leuven; K. Abrahams and P. Van Assche (eds.), Institute of Physics, Bristol and Philadelphia, Conference Series n° 88 (1988), p. 461

ROHR, G.
Doorway structures in ^{28}Si+n and ^{32}S+n based on discontinuities of the level spacing.
Ibidem, p. 643

ROHR, G.
New aspects of nuclear level spacing distributions.
Nuclear Data for Science and Technology, Proc. Intern. Conf., Mito; S. Igarasi (ed.), JAERI, Tokyo (1988), p. 707

ROHR, G., SHELLEY, R., BRUSEGAN, A., POORTMANS, F., MEWISSEN, L.
Discontinuities in the level spacings observed with ^{52}Cr+n resonances.
Ibidem, p. 779

ROHR, G., SHELLEY, R., MEWISSEN, L., POORTMANS, F.
Gaussian-like distribution of neutron resonance levels.
Frühjahrstagung des Fachausschusses Kernphysik der DPG, Berlin, March 21-25, 1988; Verhandlungen DPG 6 (1988) C9, 1

ROHR, G., SHELLEY, R., VANPRAET, G.
Nuclear energy level spacing distributions in even iron isotopes.
Nuclear Data for Science and Technology, Proc. Intern. Conf., Mito; S. Igarasi (ed.), JAERI, Tokyo (1988), p. 787

SOWERBY, M.G., CORVI, F.
Matters related to the NEANDC task forces on ^{235}U and ^{56}Fe resonances.
Nuclear Data for Science and Technology, Proc. Intern. Conf., Mito; S. Igarasi (ed.), JAERI, Tokyo (1988), p. 37

WAGEMANS, C., DERUYTTER, A.J., BARTHELEMY, R., MAMPE, W., AGERON, P., MICHAUDON, A.
Investigation of the shape of the ^{235}U (n,f) cross section with very cold neutrons.
Nuclear Data for Science and Technology, Proc. Intern. Conf., Mito; S. Igarasi (ed.), JAERI, Tokyo (1988), p. 131

WAGEMANS, C., SCHILLEBEECKXS, P., DERUYTTER, A.J., BARTHELEMY, R.
Subthermal fission cross-section measurements for ^{233}U, ^{235}U and ^{239}Pu.
Ibidem, p. 91

WAGEMANS, C., WEIGMANN, H., BARTHELEMY, R.
Nuclear structure studies with (n,α) and (n,p) reactions.
Capture Gamma-Ray Spectroscopy, Proc. 6th Intern. Symp., Leuven; K. Abrahams and P. Van Assche (eds.), Institute of Physics, Bristol and Philadelphia, Conference Series N° 88 (1988), p. 739

WAGNER, M., WINKLER, G., VONACH, H., LISKIEN, H.
Measurement of the $^{93}Nb(n,n')$ ^{93m}Nb cross section at 7.9 MeV.
Nuclear Data for Science and Technology, Proc. Intern. Conf., Mito; S. Igarasi (ed.), JAERI, Tokyo (1988), p. 1049

WEIGMANN, H.
Summary on nuclear structure at high excitations and nuclear reactions.
Capture Gamma-Ray Spectroscopy, Proc. 6th Intern. Symp., Leuven; K. Abrahams and P. Van Assche (eds.), Institute of Physics, Bristol and Philadelphia, Conference Series N° 88 (1988), p. 435; J. Phys. G, Nucl. Phys. 14 Suppl. (1988) S435

WEIGMANN, H., KÖHLER, R., POORTMANS, F., RAMAN, S., WARTENA, J.A.
Ground state partial radiative widths of ^{207}Pb+n resonances and M1 and M2 strengths in ^{208}Pb.
Capture Gamma-Ray Spectroscopy, Proc. 6th Intern. Symp., Leuven; K. Abrahams and P. Van Assche (eds.), Institute of Physics, Bristol and Philadelphia, Conference Series N° 88 (1988), p. 655

WEIGMANN,H., MARTIN, P., POORTMANS, F., WARTENA, J.A.
Ground state partial radiative widths of ^{28}Si+n resonances.
Ibidem, p. 625

SCIENTIFIC OR TECHNICAL ARTICLES

BUDTZ-JØRGENSEN, C., KNITTER, H.-H.
Simultaneous investigation of fission fragments and neutrons in ^{252}Cf(SF).
Nucl. Phys. A490 (1988) 307

CORVI, F., PREVIGNANO, A., LISKIEN, H., SMITH, B.P.
An experimental method for determining the total efficiency and the response function of a gamma-ray detector in the range 0.5 - 10 MeV.
Nucl. Instr. Methods Phys. Res. A265 (1988) 475

D'EER, A., WAGEMANS, C., NEVE DE MEVERGNIES, M., GÖNNENWEIN, F., GELTENBORT, P., MOORE, M.S., PAUWELS, J.
Neutron induced fission of the 26 min uranium-235 isomer.
Phys. Rev. C 38 (1988) 1270

HAMBSCH, F.J., KNITTER, H.-H., BUTDZ-JØRGENSEN, C., THEOBALD, J.P.
Fission mode fluctuations in resonances of ^{235}U(n,f).
Nucl. Phys. A491 (1989) 56

KLOPF, P. (†), STÜBER, W.
A linear mixer and shape normalizer for 50 ms tail pulses.
Nucl. Instr. Methods Phys. Res. A (to be published)

KNITTER, H.-H., BUTDZ-JØRGENSEN, C.
Neutron induced fission cross section of ^{243}Am in the energy range from 1 MeV to 10 MeV.
Nucl. Sci. Eng. 99 (1988) 1

LISKIEN, H., WIDERA, R., WÖLFLE, R., QAIM, S.M.
Experimentally determined excitation function for the ^{9}Be(n,t) reaction.
Nucl. Sci. Eng. 98 (1988) 266

LIU, X.D., BABELIOWSKY, T.
APL in a chemical application - processing of spark source cross spectrometry data.
Trends in Anal. Chem. (to be published)

PAUWELS, J.
Nickel metal for reactor neutron dosimetry - EC Nuclear Reference Material 521.
EUR - 11689 EN (1988)

RYVES, T.B.
A simultaneous evaluation of some important cross sections at 14.70 MeV.
EUR - 11912 EN (1988); European Appl. Res. Reports, Nucl. Sci. and Techn. Sect. (to be published)

WÖLFLE, R., MANNAN, A., QAIM, S.M., WIDERA, R., LISKIEN, H.
Excitation functions of $^{93}Nb(n,2n)^{92m}Nb$, $^{93}Nb(n,\alpha)^{90m,g\gamma}$, $^{139}La(n,\alpha)^{136}Cs$ and $^{181}Ta(n,p)^{181}Hf$ reactions in the energy range of 12.5 to 19.6 MeV.
Appl. Radiat. Isot., Int. J. Radiat. Appl. Instrum. Part A 39 (1988) 407

SPECIAL PUBLICATIONS

HANSEN, H.H. (ed.)
Annual Progress Report on Nuclear Data 1987.
NEANDC (E) 292 "U", Vol. III Euratom; INDC (EUR) 022/G (1988)

GLOSSARY

A E C L	Atomic Energy of Canada Limited, Chalk River (CND)
A E R E	Atomic Energy Research Establishment, Harwell (GB)
B I P M	Bureau International des Poids et Mesures, Sèvres (F)
B N F L	British Nuclear Fuel Limited, Windscale (GB)
C B N M	Central Bureau for Nuclear Measurements (JRC-Geel), Geel(B)
C C E M R I	Comité Consultatif pour les Etalons de Mesure des Rayonnements Ionisants
C E A	Commissariat à l'Energie Atomique, Paris (F)
C E C	Commission of the European Communities
C E N	Centre d'Etudes Nucléaires, Saclay (F)
C I E M A T - J E N	Centro de Investigacion Energetica Medio Ambiental y Tecnologia - Junta de Energia Nuclear, Madrid (E)
C M	Centre of mass
C N E N	Comissão Nacional de Energia Nuclear, Rio de Janeiro (Brazil)
C R P	Coordinated Research Programme
C S R S R	Centre for Standardisation and Radiological Safety Research, Jakarta (RI)
D P G	Deutsche Physikalische Gesellschaft
E C	European Community
E C N	Energieonderzoek Centrum Nederland, Petten (NL)
E N D F	Evaluated Nuclear Data File
E N E A	Comitato Nazionale : Energia Nucleare e Energia Alternative
E T L	Electrotechnical Laboratory, Ibaraki (Japan)
E W G R D	European Working Group on Reactor Dosimetry
G D	General Direction
G E L I N A	Geel Electron Linear Accelerator
I A E A	International Atomic Energy Agency, Vienna (A)
I C R M	International Committee for Radionuclide Metrology
I C S T I	International Centre for Scientific and Technical Information, Moscow (SU)
I E A	Instytut Energii Atomowej, Swierk (PL)
I L L	Institut Laue-Langevin, Grenoble (F)
I M M	Institut de Métrologie D.I. Mendéléev, Leningrad (SU)
I N D C	International Nuclear Data Committee
I R K	Institut für Radiumforschung und Kernphysik, Wien (A)
J A E R I	Japan Atomic Energy Research Institute

J E F	Joint European File
J E N D L	Japanese Evaluated Data Library
J R C	Joint Research Centre
K F A	Kernforschungsanlage, Jülich (D)
K F K	Kernforschungszentrum Karlsruhe, Karlsruhe (D)
L M R I	Laboratoire de Métrologie des Rayonnements Ionisants, Saclay (F)
N A C	National Accelerator Centre, Faure (F)
N B S	National Bureau of Standards, Gaithersburg (USA)
N E A	Nuclear Energy Agency, Paris (F)
N E A N D C	Nuclear Energy Agency's Nuclear Data Committee
N I M	National Institute of Metrology, Beijing (PR of China)
N I S T	National Institute of Standards and Technology, Gaithersburg (USA)
N P L	National Physical Laboratory, Teddington (GB)
N R C	National Research Council of Canada, Ottawa (CND)
O M H	Orzágos Mérénigyi Hivatal, Budapest (H)
O R N L	Oak Ridge National Laboratory, Oak Ridge (USA)
P T B	Physikalisch-Technische Bundesanstalt, Braunschweig (FRG)
S C K/ C E N	Studiecentrum voor Kernenergie/ Centre d'Etudes Nucléaires, Mol (B)
S I R	Système International de Référence
T O F	Time of Flight
U K A E A	United Kingdom Atomic Energy Authority
U V V V R	Ústavu pro Výzkum, Výrobu a Využiti Radioisotope, Prague (CS)
W R E N D A	World Request List for Neutron Data Measurements

CINDA ENTRIES LIST

ELEMENT		QUANTITY	TYPE	ENERGY		DOCUMENTATION		LAB	COMMENTS
S	A			MIN	MAX	REF VOL PAGE	DATE		
U	235	NF	EXPTL-PROG	60-4	13+1	INDC(EUR)023G003	-89	GEL	KNITTER + LINAC MASS DIST.
CF	252	SNF	EXPTL-PROG			INDC(EUR)023G004	-89	GEL	BROSA + FISS. PROD. MASS DIST.
U	233	NF	EXPTL-PROG	10-3	10+0	INDC(EUR)023G010	-89	GEL	WAGEMANS + LINAC WESTCOTT FACTORS
U	235	NF	EXPTL-PROG	10-3	10+0	INDC(EUR)023G010	-89	GEL	WAGEMANS + LINAC WESTCOTT FACTORS
PU	239	NF	EXPTL-PROG	10-3	10+0	INDC(EUR)023G010	-89	GEL	WAGEMANS + LINAC WESTCOTT FACTORS
U	235	ETA	EXPTL-PROG			INDC(EUR)023G014	-89	GEL	WEIGMANN + ILL HFR
U	238	NG	EXPTL-PROG	20-4	10-1	INDC(EUR)023G015	-89	GEL	CORVI + LINAC
U	235	NF	EXPTL-PROG	10-6	10-5	INDC(EUR)023G018	-89	GEL	WAGEMANS + ILL HFR
PU		SNF	EXPTL-PROG			INDC(EUR)023G018	-89	GEL	SCHILLEBEECKX + SHELL EFFECTS
FE	056	NG	EXPTL-PROG	11+3	11+3	INDC(EUR)023G021	-89	GEL	CORVI + REVIEW OF RES. TASK FORCE
MO		NA	EXPTL-PROG	12+7	20+7	INDC(EUR)023G026	-89	GEL	LISKIEN + VDG EXCITATION FUNCTION
CR	052	N2N	EXPTL-PROG	12+7	20+7	INDC(EUR)023G027	-89	GEL	LISKIEN + VDG EXCITATION FUNCTION
NI		NA	EXPTL-PROG	14+7	14+7	INDC(EUR)023G028	-89	GEL	WATTECAMPS VDG RATIO TO NI58
CU		NA	EXPTL-PROG	14+7	14+7	INDC(EUR)023G028	-89	GEL	WATTECAMPS VDG RATIO TO NI58
CR	050	NG	EXPTL-PROG	10+3	10+6	INDC(EUR)023G033	-89	GEL	ROHR + LEVEL DENSITY
CR	052	RES	EXPTL-PROG	10+3	10+6	INDC(EUR)023G033	-89	GEL	ROHR + LEVEL DENSITY